AN ABSTRACT OF THE THESIS OF

Jeffrey A. Fantozzi for the degree of Master of Science in Forest Products presented on April 18, 1988.

Title: Tensile Failure Characteristics of Bolted Wood Joints Subjected to Bending Moments

Signature redacted for privacy.

Abstract approved _____
Dr. Philip E. Humphrey

Traditionally, bolted joints have been designed to carry unidirectional loads. We have little knowledge about the effects of combined loading on the failure characteristics of joints with more than one bolt. In this thesis, two techniques are presented which enable such joints to be evaluated when they are subjected to a combination of tensile and bending forces.

Firstly, a two-dimensional technique was developed. This involved placing specially prepared thin wafers of wood between two rigid Plexiglas plates. Steel pins passing through the Plexiglas-wafer assembly were used to represent bolts. Two bolt configurations and two grain orientations were investigated using the technique. Wafers were first tested to failure under tensile forces only, and following this, a series of tests were conducted in which combined tensile and bending forces were applied to wafers. Load-slip curves and visual observation of in-plane failure

modes were used to determine the effects of combined loading on the behavior of the simulated joints.

Results from preliminary tests using this technique suggest that bending moments can indeed significantly reduce the tensile strength properties of joints, and that the arrangement of bolts influences failure characteristics. A modified joint design (triangular bolt arrangement) appeared to be less susceptible to bending moments than the conventional design (three bolts in a line).

Tests were also carried out on complete joints of conventional design (three bolts in a line). This was in order to evaluate the results from the wafer technique, and also to gain empirical information on the vulnerability of existing joint designs to combined loading. Results of the two-dimensional tests of the modified design were encouraging and full scale tests on complete joints with this new design are now considered warranted.

Tensile Failure Characteristics of Bolted Wood Joints Subjected to Bending Moments

By

Jeffrey A. Fantozzi

A THESIS

submitted to

Oregon State University

in partial fulfillment of
the requirements for the
degree of

Master of Science

Completed April 18, 1988

Commencement June 1989

APPROVED:

Signature redacted for privacy.

Dr. Philip E. Humphrey
Professor of Forest Products in charge of major

Signature redacted for privacy.

Dr. Robert Ethington
Head, Department of Forest Products

Signature redacted for privacy.

Dr. John Ringle
Dean of Graduate School

Date Thesis is presented April 18, 1988

ACKNOWLEDGMENTS

I would like to thank those friends who encouraged supported me throughout this project, especially Dr. Philip Humphrey for his patient prodding and good advice, Dr. Helmuth Resch for extending my financial support, and Keith Lanning for allowing me to use the facilities of the California Redwood Association. To my family and Karen, who remained understanding, helpful and who put up with me in general, you're the best.

TABLE OF CONTENTS

LIST OF FIGURES

LIST OF TABLES

TENSILE FAILURE CHARACTERISTICS OF BOLTED WOOD JOINTS SUBJECTED TO BENDING MOMENTS

Chapter I

BACKGROUND TO THE RESEARCH

1.1 BACKGROUND

Most structures are fabricated from individual components which are connected together to form complete working systems. In structural applications, the stiffness and strength of such connections are important considerations in the design of the structure. Joints between structural members must be able to effectively transfer loads from one member to another while at the same time preventing excessive deflection. Hence, they must provide sufficient strength and stiffness to the system. These connections can often play a greater role in determining the performance of a structure than the mechanical and physical properties of the structural members themselves.

Since wood has remained an important structural material throughout history, a wide range of wood fasteners have evolved. The type of fastener chosen for a particular application is often a function both of economics and strength and stiffness requirements. Nails and screws may be adequate for light frame construction. Where large

loads are expected, however, bolts, plates and hangers may be combined to achieve the required joint strength.

Engineered to resist large tensile loads in heavy construction applications, bolts are a widely used method of connecting wood members of structures. The construction of such joints can vary in several ways, namely: the type of material used to manufacture the members (usually wood or steel), the number and size of bolts used and the geometrical arrangements of the bolts in the members.

In the United States, the National Forest Products Association (NFPA) publishes National Design Specifications (NDS) which contain rules and guidelines for the design of wood structures. The NFPA has related some of the aforementioned variables, along with wood species and grain direction, to joint performance. Large safety factors can lead to overdesigned joints. This in turn increases construction costs and weakens the position of wood-based products in the structural market.

On the other hand, based on recent empirical work, the 1982 edition of the NFPA NDS (15) contains revisions which permit significant increases in the design values for bolted joints in certain circumstances. These revisions have been questioned by some engineers who feel that the new design values may result in underdesigned joints which could fail in service. This relates particularly to large bolt diameters.

Clearly, there is a need for fundamental information on the factors which influence performance. Aside from the empirical tests which have been carried out on standard joints, little is known regarding the effects of such factors as combined loading and bolt configurations on the integrity of bolted members.

1.2 GOALS OF THE PRESENT RESEARCH

This study is focused primarily on learning more about the performance of multiple bolted joints when both axial forces and bending forces are applied. The study has been limited to tensile axial forces; it has not considered compression. With some modifications, the methods used could be extended to include compression, however.

Two complementary techniques have been used. Firstly, a two dimensional approach, similar to that developed by Ostman (18) but considerably extended, was used to study joint failure mechanics. This method utilizes thin wafers supported on both faces by transparent, rigid plates to model one member of a bolted joint. Steel pins traveling through the sandwich assembly are used to represent bolts. In-plane forces applied between the wafer and the restraining plates represent loading of the corresponding joint. To complement this technique, full scale joint testing was also performed. Both methods involved the application of bending forces and tensile forces to the joint or wafer-pin system under test.

1.3 METHOD OF REPORTING USED IN THE THESIS

The thesis is divided into seven chapters. Relevant literature will be discussed in chapter II. The general principles involved in the two techniques used will be described in chapter III. Chapters IV and V consider each technique in detail. They can be thought of as paralleling one another as they contain similar sub-divisions. Chapter VI is a discussion of the results. Conclusions and recommendations for future research are made in chapter VII. The appendices contain a copy of the computer program utilized in this research along with analysis of variance tables.

A note about units of measurement is appropriate here. To simplify analysis, Systems International (SI) units are used throughout the thesis. Bolt and joint measurements are, however, recorded in inches and simple fractions of inches. This is to enable comparisons to be made with the results of previous researchers who mainly worked in inches.

Chapter II

CRITICAL DISCUSSION OF THE LITERATURE

2.1 INTRODUCTION

The majority of work on bolted joint connectors has been based on empirical approaches using complete joints. Unfortunately, those methods do not always provide us with the insight needed to efficiently design joints based on thorough understanding. Information obtained from this approach is specific to the particular experimental configuration tested. Nevertheless, the best method to verify the reliability of joint designs is to test complete joints. The development of designs is, however, best approached fundamentally.

Before the past research is discussed, it will be helpful to define some of the more common terms used to describe such joints. Figure 2.1 has been included for this purpose.

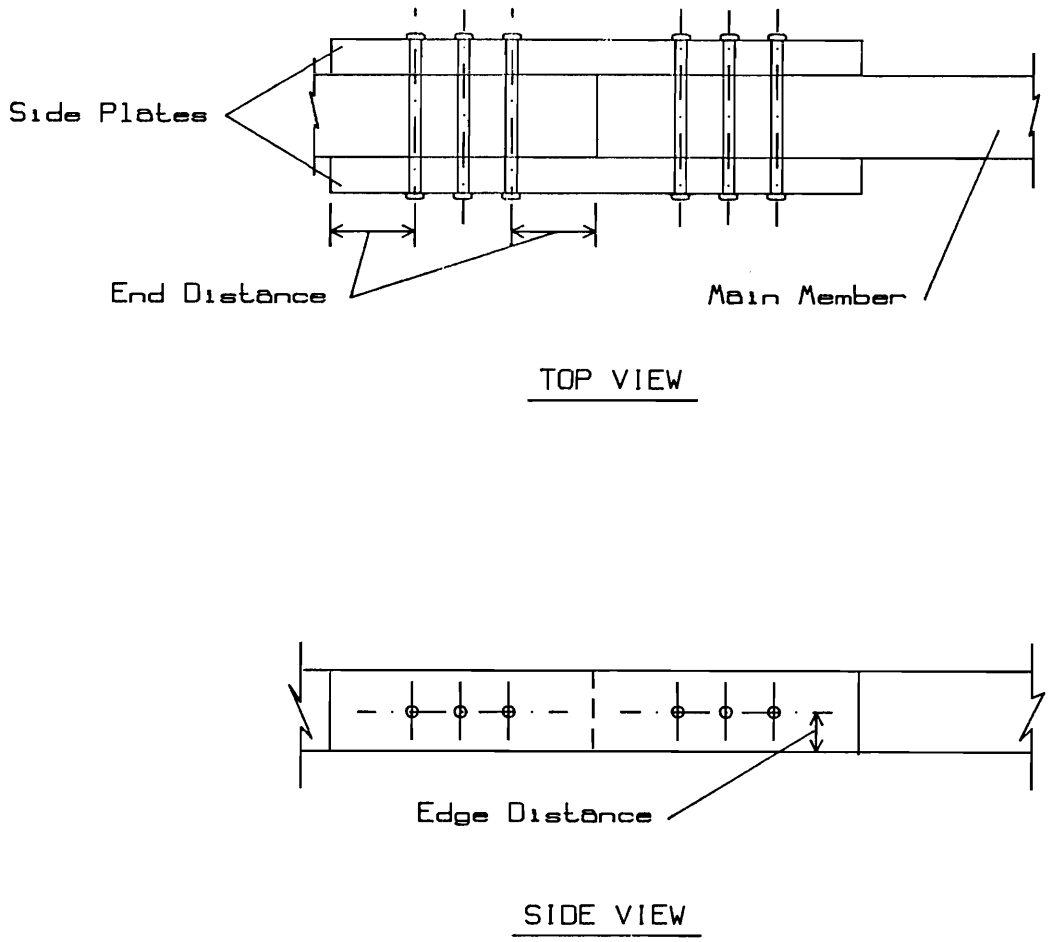

Figure 2.1 Schematic representation of some common terms used when specifying bolted joints

G.W. Trayer (25) was among the first to experimentally test bolted joints used in wood structures. In his original work, Trayer tested hundreds of bolted joints using both metal and wooden side plates while varying the diameter, length and bolt spacing. Many design specifications (eg. 7 bolt diameter end distance, 25% load increase when using steel side plates rather than wood) have been based on the results of his work. More recent research,

however, has been interpreted as suggesting that some generally accepted design values are in need of modification.

2.2 SINGLE BOLT JOINTS

In 1960, Snodgrass and Gleaves (23) tested nearly 500 single bolt joints in double shear to examine the effects of seasoning, end distance, grain direction and L/D ratios (the ratio of bolt length to bolt diameter). Their results suggest, among other things, that reductions in end distances to 4 bolt diameters would not significantly reduce the load at proportional limit (p.l.)[1] for this type of joint. Their investigation also indicates that the designer faces unnecessarily severe reductions in allowable loads when unseasoned wood is used.

Wilkinson and Rowlands (29) reported on work combining numerical and experimental approaches. These were used to analyze the plane stresses and strains developed in the wood material caused by load transfer of the bolt. Strain gauges and moire fringe patterns were used in the experimental study, while finite element analysis was used in the numerical models. An objective of these techniques was to

[1] The exsistance of a true proprtional limit in a complex system such as a bolted joint is questionable because of the interaction of the various components involved. The term will be used here, however, when other researchers have referred to it.

evaluate the effects of end and edge distances, inter-member friction and the ratio of pin-to-hole diameter on stress distribution. The results suggest an optimal end distance of 8 bolt diameters (in contrast to the findings of previously mentioned researchers). The study also indicated that small variations in the ratio of pin-to-hole diameters had a significant effect on localized stress concentrations and that friction between the pin and wood hole surfaces also had considerable influence.

In 1980, separate reports by Wilkinson (26) and Thangjitham (24) indicated that when using metal side plates, the allowable load may be greater than that proposed by Trayer. Working from this, McLain (14) tested nearly one hundred joints using single 1/2" diameter bolts. The results suggest that when metal side plates are used with 1/2" diameter bolts, an increase in the load at proportional limit may be justified. Largely based on McLain's work, the 1982 edition of the NDS includes an increases of 75% in allowable load when metal side plates are used. The previously accepted figure in the NDS was 25%, based on Trayer's work. While this dramatic increase appears to benefit the financier, it has also generated some controversy, particularly in the light of a number of serious structural failures that have occured.[2]

[2] The 1986 edition of the NDS has been modified to reflect some of these concerns. Increases in allowable loads are now dependent on bolt diameter.

2.3 MULTIPLE BOLT JOINTS

Several researchers have considered joints fabricated with multiple bolts placed in rows parallel to the loading direction. (3,4,5,11,12,13,25,26,27,28). Lantos (13) and Cramer (3) developed similar methods to determine the load distribution among a row of bolts. Cramer's method allows for nonuniform stress distribution in the members and uses the bearing stress distribution to determine the joint slip modulus. From these techniques, modification factors can be derived which are used in the calculation of the allowable joint load. The modification factors that appear in the current NDS edition are based on the Lantos method of calculating load distribution. Wilkinson (26) evaluated the effects of several joint variables on these modification factors. In this report, he concluded that the current methods were adequate to predict the load at proportional limit, but they failed to estimate the ultimate load of joints.

The methods described above did not consider the effect of fabrication tolerances or variable load-slip behavior between bolts in a row. The significance of these factors was implied by Dannenberg and Sexsmith (4). In 1983, Wilkinson (27,28) experimentally measured the stresses and strains of individual bolts in several joint geometries to determine the effects of these factors. Using the load-slip curves from each bolt, a numerical method for

determining load distribution among individual bolts was developed. From this data, computer simulation was used to randomly generate load-slip curves of individual bolts. These curves were then used in a model to predict the proportional limit and ultimate strength of bolted joints made using 5 bolts per row. This method resulted in a distribution of randomly generated modification factors which could be used in the allowable load calculations.

While the above modeling approach may prove applicable in the long term, more realistic results will depend on our developing approaches which enable us to see the true behavior of the joint throughout its complete loading cycle.

Many studies have looked at single bolt joints and load distribution of multiple bolts in a row; few have examined the effects of bolt configuration on joint properties. One such empirical study by Kunesh and Johnson (12) suggested that bolt patterns had a significant effect on the bearing capacity of a joint at both proportional limit and maximum load. They went further to say that staggering the rows resulted in a higher load carrying capacity than if the bolts were placed in vertical or horizontal rows, and that this was dependent on the number of double shear areas between the rows. These conclusions, which are supported by the present study, stand in contrast to those suggested by Trayer.

2.4 COMBINED LOADING MODES

Traditionally, bolted joints have been designed to carry purely axial (tensile or compressive) loads. Naturally, the overwhelming majority of bolted joint research only involves testing in these modes. In service, however, a joint may experience a combination of axial (tensile) and non-axial (bending) forces. These bending forces may be the result of non-ideal design, structural settling, or the weight of heavy members. Rigid connections, such as those formed when multiple bolts are used, will resist bending moments. This can be of particular importance when a system, such as a frame, is subject to racking forces.

The effects of such bending moments on the performance of bolted joints are not well understood. Several researchers have looked at the effects of combined loading on structural lumber using bending and compression loads (2,10,16,17,19,30). Wood subjected to such loading was assumed to conform to the simple linear interaction equation which states that the stress at any point in a cross-section is equal to the sum of the imposed stresses. When the sum of these stresses exceeds the allowable stress for a member, failure occurs.

Senft and Suddarth (21) reported on the strength of dense 2" X 4" southern pine under combined bending and tensile loads. Their technique was to apply a tensile

force to a member and then increase the bending load until failure occurred. Throughout the test, they maintained the tensile force within 2% of its original value. Their data did not support the interaction equation.

Later, Senft (20) reported on a similar study using 2" X 4" western hemlock and came up with similar results. Under combined loading, the bending load at the time of failure was nearly independent of the applied tensile load. Senft suggested that the effect of the counter moment produced by the tensile load acting through the deflected specimen shifted the stress in the member. By including the bending stresses caused by this resisting moment, Senft was able to use the traditional interaction equation to determine the allowable load with favorable results.

Recently, there has been a shift in design philosophies towards the interaction of individual components in systems such as floors, walls or roofs (6,7). This "systems" approach offers increased efficiency and economy while at the same time providing the designer with meaningful means of analysis. To fully utilize this design approach, a more fundamental understanding of joint response to various load conditions is necessary. Very recent studies have taken some strides in this direction.

In 1984, Hirai (8) reported on the effect of loading direction (angle between the loading direction and the grain direction) on the bearing properties of wood under a bolt. His results showed that within the elastic range,

the proportional limit load increased as load direction approached the parallel to grain condition. Another report by Hirai and Horie (9) discussed the effects of loading direction on the lateral resistance of single bolt joints made with steel side plates. The results suggest that when loaded perpendicular to the grain, the load at proportional limit was approximately two-thirds of that when loaded parallel to the grain. Maximum load perpendicular to the grain was approximately 27% of the maximum load parallel to the grain.

These studies are tenuously related to the issue of bending moments in joints but they do not address it directly.

Fundamental methods of design may also aid in our developing new connector systems to complement new structural systems and materials. These could potentially include composite materials formed into a wide range of fabricated or molded structural members and modules.

Initial work aimed at meeting these objectives has been reported by Ostman (18) in his thesis "Development of Techniques to Study the Behavior of Bolted Wood Joints". Ostman's research furnishes some of the approaches used in this research. It did not, however, concern itself with many of the variables which affect joint strength. To gain a more complete understanding of joint behavior as it is affected by the important factors of bending moments and bolt configuration, the present investigation is necessary.

Chapter III

THE PRINCIPLES OF THE TWO TECHNIQUES

3.1 SPECIFIC OBJECTIVES OF THE RESEARCH

The primary objectives of this work fall into four main categories:

1) Improvement and refinement of the aforementioned wafer technique for studying wood deformation within joints during loading.

2) Consideration of the complex behavior of multiple bolt joints by using the wafer technique, especially under combined loading conditions.

3) Comparison of observations made using the wafer technique with information gained by testing whole joints under corresponding loads.

4) Preliminary evaluation of a new bolt configuration using the wafer technique.

Figure 3.1 shows a flow diagram representing the work plan that was followed. In this preliminary work, one joint construction (with respect to member sizes and bolt configuration) was established as a "standard". The performance of these joints provides a reference against which other types of joints can be evaluated. The nature of relationships between design factors which are common to all joints may be determined by investigation of such a standard.

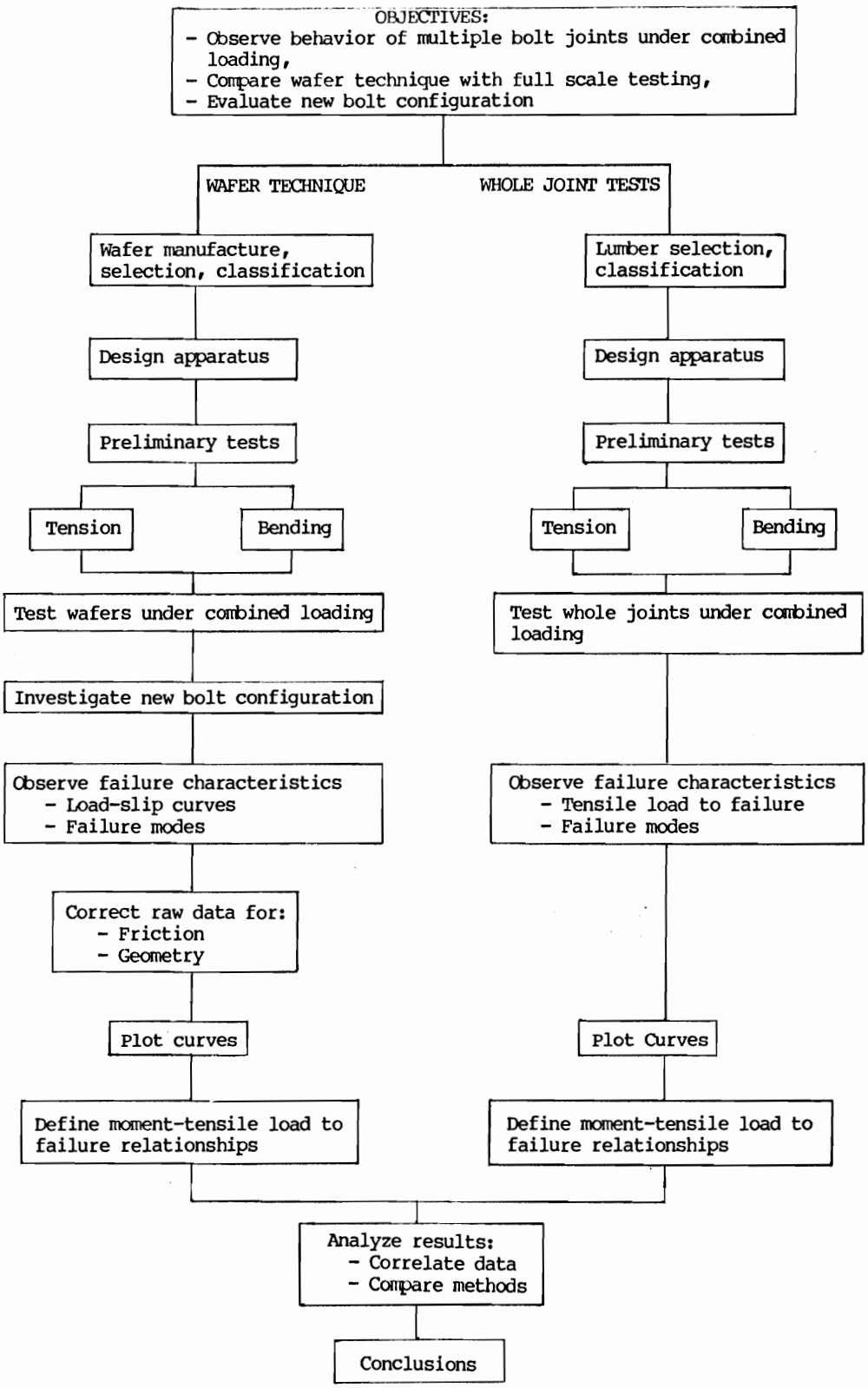

Figure 3.1 Flow diagram of the workplan followed in this study

Figure 3.2 shows the joint design established as the standard for the present work. A three member joint was chosen because it is one of the more common constructions used. Wood side plates were used because the design values for steel side plates has been questioned; metal plates will be tackled once the ground work is complete.

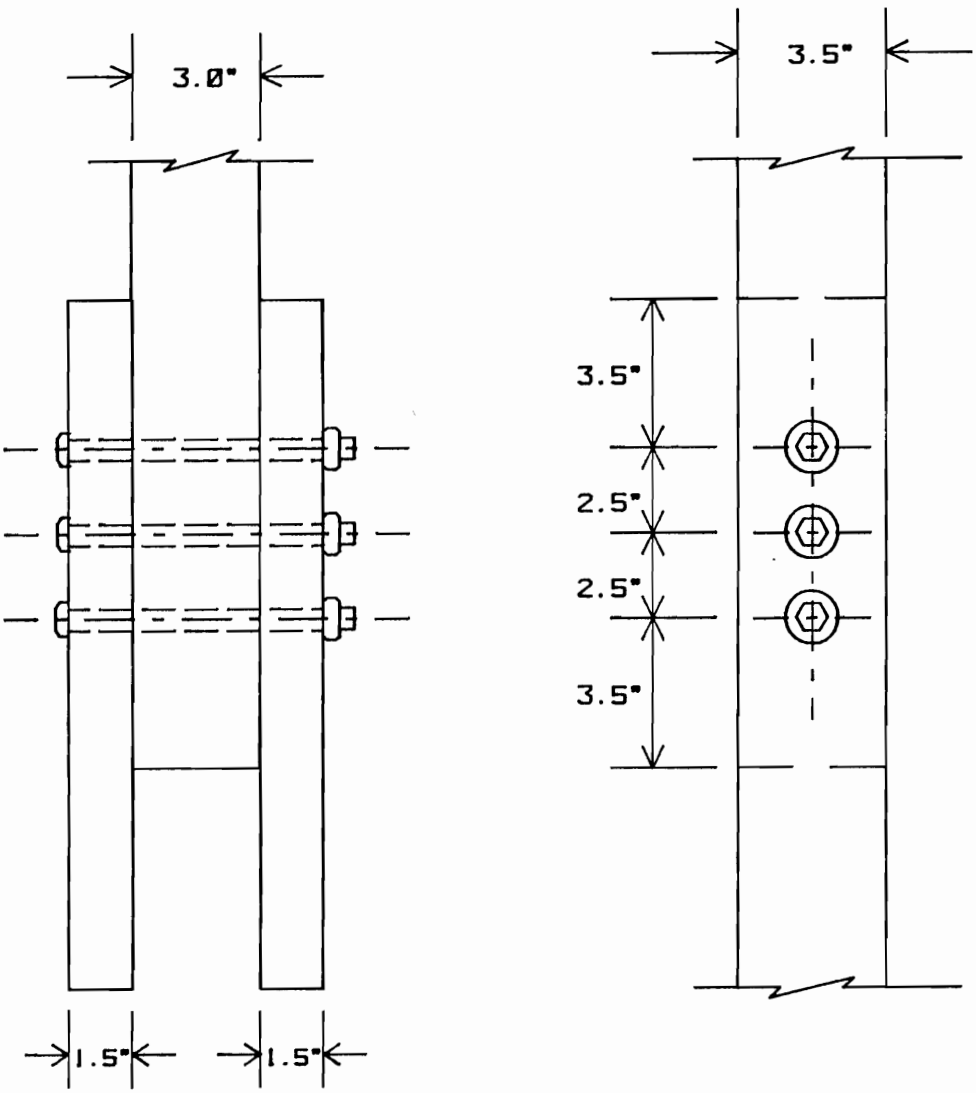

Figure 3.2 The standard joint design

The joint consists of a 3" X 3 1/2" wood main member and two 1 1/2" X 3 1/2 " wood side members. The members are connected together by three 1/2" diameter steel bolts located in a single row and spaced according to the 1982 NDS standards (15). This is a common bolt configuration for which modification factors have been developed (28).

To model the full size joint using the wafer technique, a corresponding "standard" wafer was defined. These wafers had the same width and bolt pattern as the full size joint. In this way, direct comparisons could be made between the two methods.

3.2 PRINCIPLES OF THE WAFER TECHNIQUE

A thin wafer of wood, when sandwiched between two smooth rigid plates, behaves in many respects as though it is part of a solid piece of lumber. This is to say that the restraining boundary material simulates a continuum of wood extending infinitely beyond the surfaces of the wafer. By using a clear material such as Plexiglas or glass for this, failure mechanisms that occur within one of the members of a bolted joint during in-plane loading may be viewed and numerical results may be obtained.

This is a two dimensional approach to a three dimensional problem. By eliminating the third dimension (parallel to the bolt axis), not only can material behavior be observed, but a reduction in complexity and associated variabilty can be achieved. This simplification can

streamline the analysis, provided that the continuum principle is obeyed. In addition, wafers require less raw material to produce and are less expensive and easier to handle than full size joints. As a result, this method may increase our efficiency in arriving at optimal joint designs.

On the other hand, the 2-dimensional approach can not completely describe the full scale joint; it can only serve as a method for evaluating some failure mechanisms. Analysis of a real 3-dimensional joint involves complex interactions between the bolt and wood materials, as shown by Ostman's work (18). Future work will involve integration of the 2-dimensional data to produce models of whole-joint behavior.

Figure 3.3 shows some of the main parts of the experimental arrangement. 1/2" diameter steel pins (which represent portions of bolts) were inserted into aligned holes drilled through both the wood and Plexiglas. The materials were kept in intimate contact by a series of regulated pneumatic clamps located around the perimeter of the Plexiglas plates.

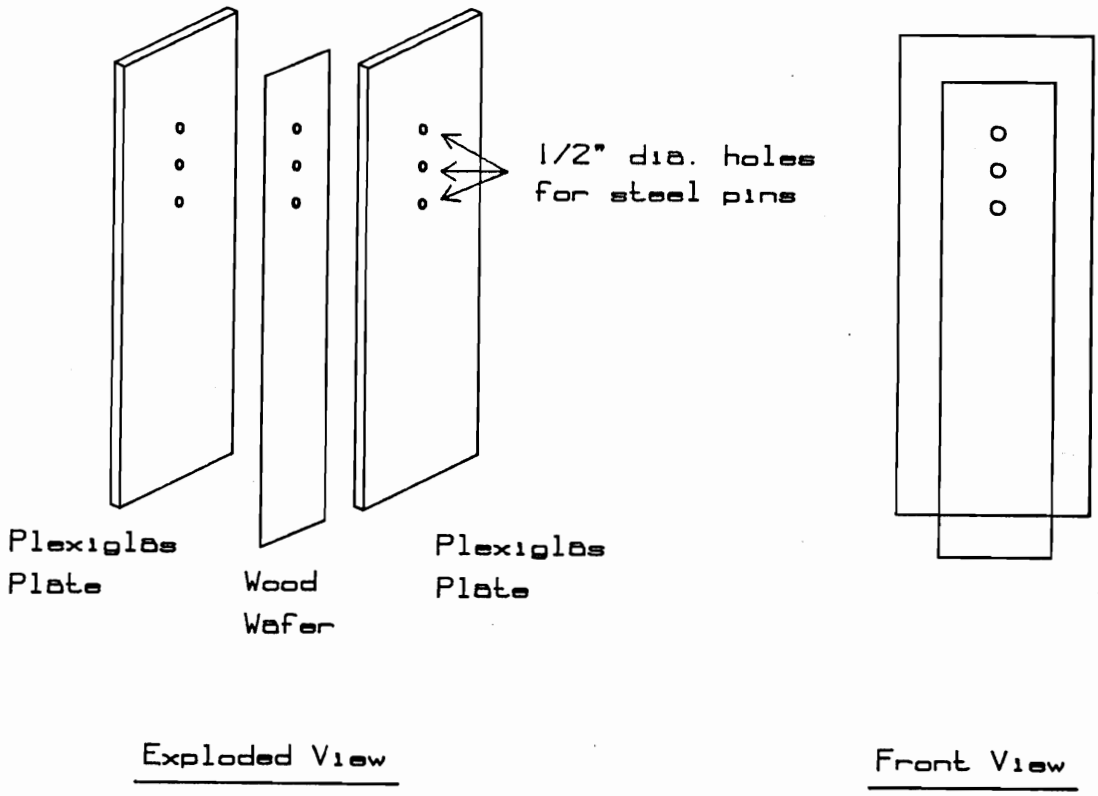

Figure 3.3 An exploded view of the wafer-plate assembly

To apply forces, the assembly was mounted on a servo-hydraulic testing machine (MTS). By restraining the Plexiglas plates laterally, forces could be applied to the bottom of the wafer where it extended beyond the plates (see Figure 3.4). The wafer was free to slide between the plates except for the resistance offered by the steel pins.

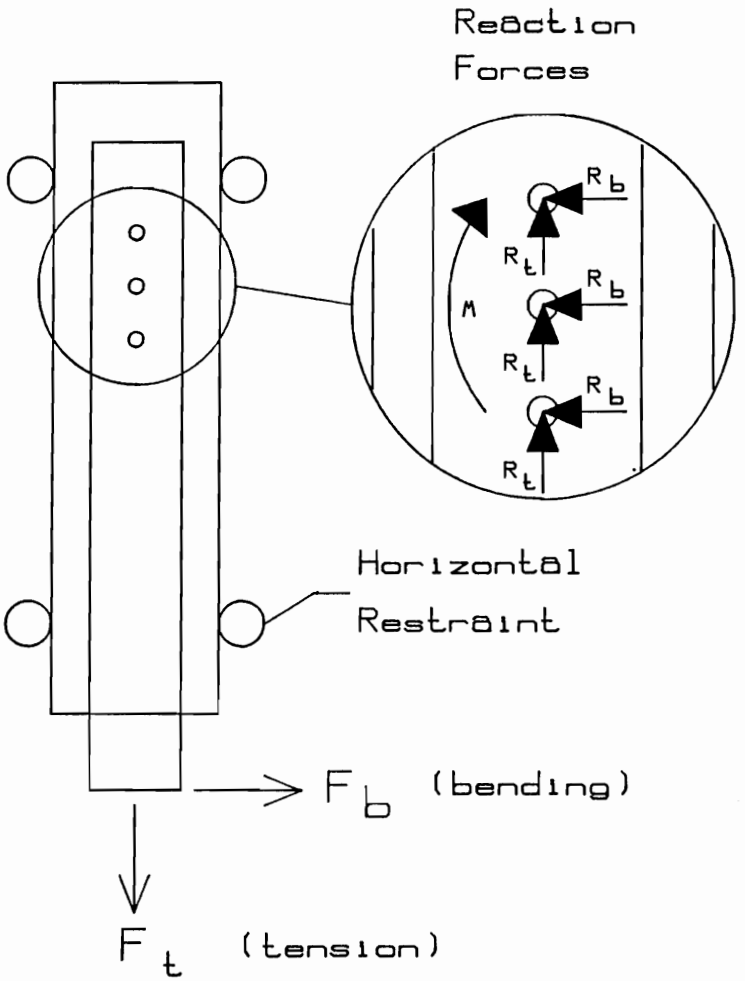

Figure 3.4 The forces acting on the wafer-pin assembly

3.3 AN OUTLINE OF TESTS ON COMPLETE JOINTS

Full scale joints were tested to establish links between the wafer approach and whole-joint tests, and to evaluate the reliability of predicted joint performance based on the wafer approach. The standard joint used in the full scale tests has been shown in Figure 3.2. Figure 3.5 shows a simple force diagram of the full scale joint under test. The main member was pin connected to the

crosshead of the 60,000 lb. universal testing machine, while the side members were pin connected to the machine's base. Tensile forces were applied by controlling the crosshead displacement. A specially designed frame equipped with a hydraulically controlled loading ram was used to simultaneously apply horizontal forces (bending moments) to the joint. The two point lateral loading produced a uniform bending moment along the length of the bolt connection itself. The geometry of this arrangement is considered fully in chapter V.

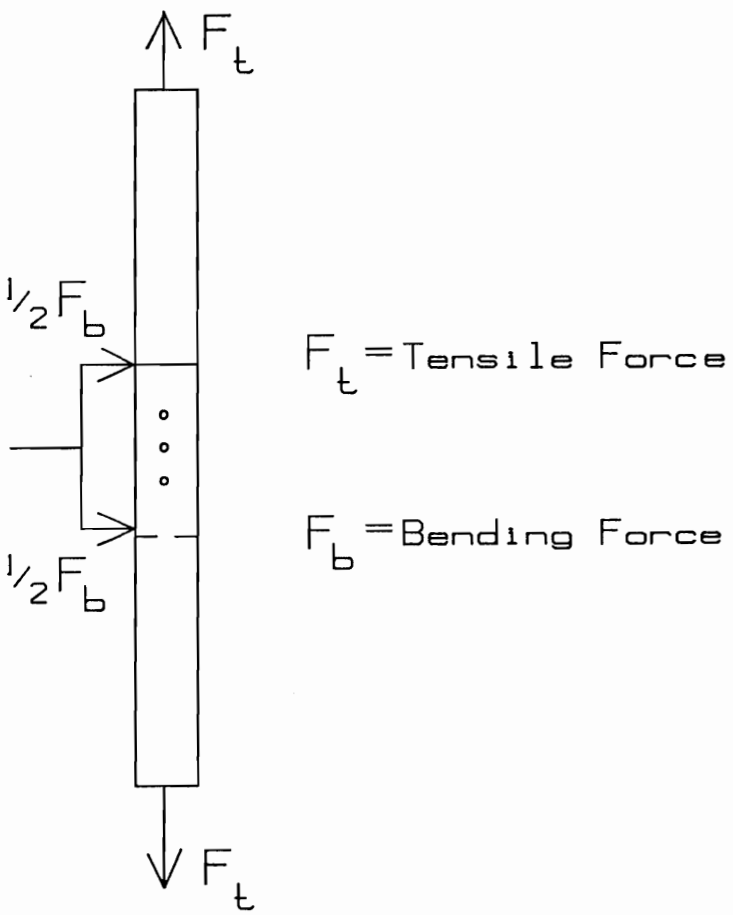

Figure 3.5 Forces applied to the full scale joints

3.4 LINKS BETWEEN THE TWO METHODS

Introduction:

Combining information gained from the wafer approach with that from full scale testing enables a more complete picture of bolted joint behavior to be formed. The wafer technique gives both numerical and visual results, and can be used as a simplified model of full scale joint behavior. Eventually, a numerical model will be developed using the data from the laminar approach with integration methods. This model will be evaluated by comparing predictions with the results of full scale tests. If it proves successful at mimicking the full scale joint, it can be used as a new tool to improve joint design.

The application of bending moments:

In both approaches, changes occur in the geometry of the joints as the tests proceed. The method adopted to account for these changes is fundamental to the evaluation of joint performance in this thesis. Applied horizontal forces cause the joint to bend. Tensile loads, however, tend to straighten the joint and thus progressively reduce the bending moment experienced by the bolt system itself. Two means of tackling this effect have been considered.

One approach was to maintain a <u>constant horizontal force</u> throughout the test. This would have resulted in bending moments in the joint which decayed as tensile forces were applied and resultant straightening

occured. Results obtained using this method would be specific to the testing geometry used in this study.

The approach used in this study was to maintain a constant bending moment on the bolt arrangement itself throughout the test. This was achieved by continuously controlling the horizontal (bending) force in a manner proportional to the applied tensile load and the angualar deflection sustained by the joint. By keeping the joint under a constant moment, the test results are not restricted to the geometry of the testing arrangement used. This was desireable because in practice, many different load conditions can produce the same bending moment.

Each of the two aspects of the work will now be considered in detail in chapters IV and V.

Chapter IV

THE WAFER TECHNIQUE - EXPERIMENTAL METHODS

4.0 INTRODUCTION

This chapter begins with a consideration of material selection and preparation. Following this, the choice of bolt configurations is discussed in the context of both the wafer and whole joint tests. Apparatus design, specific experimental methods and data reduction then follow. Data analysis and discussion will be addressed in chapter VI.

4.1 MATERIAL SELECTION AND SAMPLE MANUFACTURE

Wafer characteristics play an important role in determining the results obtained with the wafer approach. Irregularities can be either inherent in the wood material itself or they can be introduced during the manufacturing processes. When thin wafers are used, the effects of strength reducing defects and flaws are critical. For this reason, the wafer approach is particularly well-suited to study the effects of specific wood characteristics. When a whole piece of wood is tested, individual characteristics, such as knots, interact in an unidentifiable way. The wafer approach can isolate these characteristics so that their specific effects may be studied. Because this method is more sensitive to minor irregularities, the tests must be highly controlled. Considerable care was therefore taken

in the selection and manufacture of wafers.

The raw material, a Douglas-fir cant, was kindly donated by the Hull-Oaks Lumber Company. Wafers were manufactured at the Nicoli Door Company in Portland, Oregon using the parallel slicing technique. Parallel slicing has several advantages over rotary slicing or peeling for this work. The wood cant moves across the knife in a direction parallel to the grain. This minimizes surface fiber damage and results in smooth, check-free veneer.

Green wafers were placed in the conditioning room where they rapidly came to an equilibrium moisture content of 10.8%. Nominal dimensions of the wafers were 70" X 5 1/4" X .01". Table 4.1 shows the variations in thickness among the wafers used in this study together with the number of growth rings per inch.

Table 4.1. Average wafer thickness and rate of growth

	Moisture Content (%)	Wafer Thickness (mm)	Rings/Inch
Average	10.78	0.84	6.8
Standard Deviation	0.21	0.104	0.4
Total # Wafers	11	29	25

Wafers with the straightest grain and fewest defects were cut to final dimensions of 3 1/2" X 32 1/4". The length was dictated in part by the physical dimensions of the testing machine. Wafer width was chosen to correspond with the dimensions of the full-sized joint. Both radial and tangential face orientations were produced. The significance of growth ring orientations will be considered in section 4.2.

Wafers were machined to their final dimensions by clamping them in stacks of approximately 30 wafers each. The grain in each wafer ran parallel to the grain of the others in the stack. A joiner was used to bring the rigidly clamped stacks down to their final width. This resulted in uniform wafers with smooth edges and only small variations in length and width. Wafers with cracks or splits along the top ends were discarded.

Finally, 1/2" diameter holes were drilled into the wafers using a drill press fitted with a specially selected 1/2" edge cut drill bit. It was found that the outer cutting edge of this type of bit produced clean holes of accurate diameter. Hole tolerance was as close to zero as possible (less than 1/32"). While NDS standards call for a clearance of at least 1/32", this introduces another variable into the test. In the future, the technique can easily be modified to investigate the effects of bolt hole diameter.

Alignment of the holes is known to effect joint performance (28). Sufficient accuracy was achieved with the help of a specially manufactured Plexiglas template. A small clamping jig was used to keep the template and wafer in position during the drilling process.

4.2 CHOICE OF BOLT CONFIGURATIONS AND WOOD ORIENTATIONS

Two bolt configurations and two grain orientations were tested. These are represented diagramatically in Figure 4.1 (a, b and c). The bolt configuration adopted as a standard consisted of a single row of three bolts spaced according to NDS standards (NDS sections 8.5.12.1 and 8.5.14.2 (a)). Radially cut wafers were used for these tests in order to be consistent with the orientation of the members used in the full scale tests. Tests using this configuration (linear) and grain orientation (radial) are labeled "L-R" throughout this thesis.

The other configuration tested had three bolts arranged in a triangular pattern, shown in Figure 4.1 (b). These tests also employed radially cut wafers and are labeled "V-R" throughout this thesis.

To briefly look at the effect of grain orientation on joint performance, the linear bolt configuration was also tested using tangentially cut veneers. These tests have been labeled "L-T" and are shown in Figure 4.1 (c). Further discussion of these configurations appears in chapter VI.

Because a wafer is nominally 2-dimensional, it cannot represent the full spectrum of grain orientations that are present in a 3-dimensional piece of wood. In a full size member, the orientation of grain impinging on the bolt can vary along its length. This method gives information for specific orientations. In the future, variations in grain orientation along the length of bolts in a joint may be modeled using integration techniques.

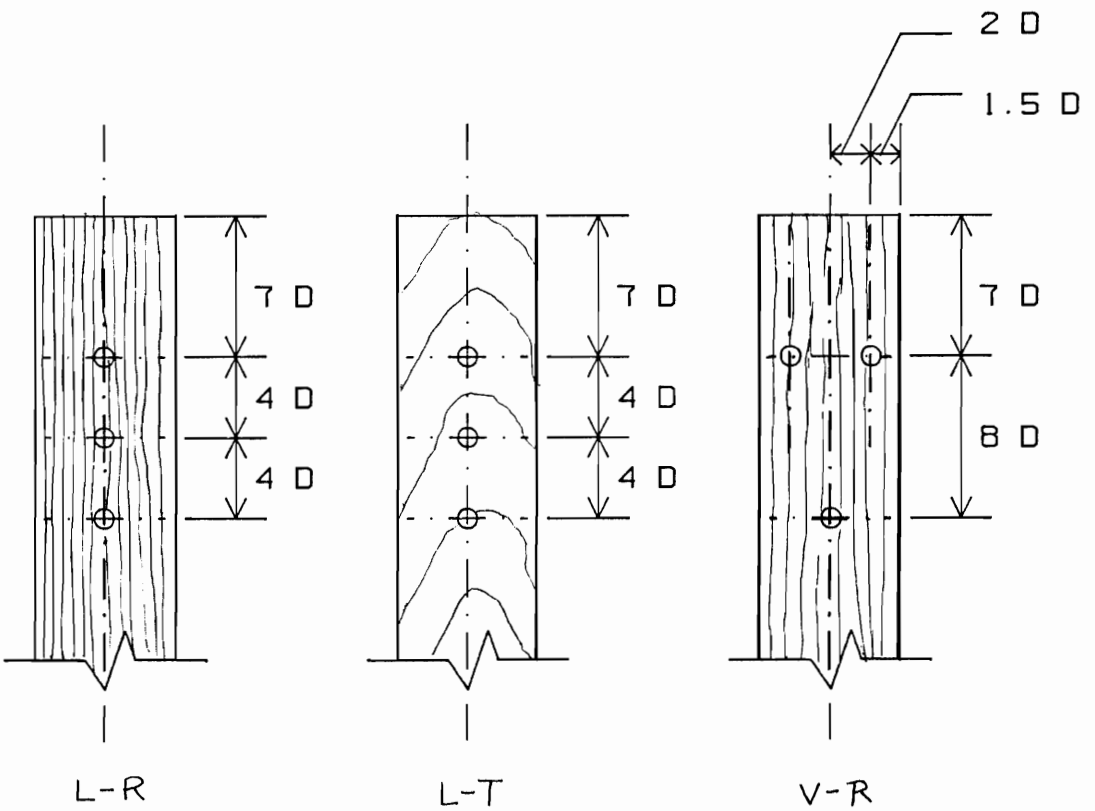

Where: D is the bolt diameter

Radial and tangential refer to the growth ring orientations of the wafers. These are a function of the cutting direction.

Figure 4.1 Bolt configurations and grain orientations employed

4.3 THE SELECTION OF BENDING MOMENT LEVELS

Preliminary tests were performed to establish the appropriate range of moment levels to be investigated. In these early tests, tensile forces were not applied to the joint; only bending loads were applied until failure occurred. Having identified the maximum bending strength of the wafer joint, six moment levels were selected to encompass bending forces from zero to the failure load. The average bending moments applied at each level prior to correcting for horizontal friction appear in Table 4.2

Table 4.2 Bending moment levels employed

Moment Level	Bending Moment Range (N m)	Identification Code		
		"L-R"	"V-R"	"L-T"
0	0	XM0	XV0	XT0
1	0*	XM1	---	---
2	0*	XM2	---	---
3	3.9 to 4.5	XM3	XV3	XT3
4	9.3 to 9.9	XM4	XV4	XT4
5	14.6 to 15.2	XM5	XV5	XT5

* After correcting for horizontal friction, bending moment equaled 0

X = replication number (1-5)

Initially, the "L-R" joints were tested using these six moment levels. After analyzing the results of these

tests, it was determined that the lower two moment levels (1 and 2) had little effect on joint performance because the applied horizontal forces were not sufficient to overcome certain forms of frictional restraint inherent in the testing arrangement. Consequently, they were not included in tests performed with "L-T" or "V-R" configurations.

4.4 THE WAFER TESTING APPARATUS

There were two main functions of the testing apparatus:

1. To provide support for the pins that represent the bolts, and to keep the spacing between them constant.
2. To restrain the wafer from moving out-of-plane.

Other requirements included:

a. the plates used to sandwich the wafer must be transparent, smooth, and rigid;
b. the wood wafer must remain in intimate contact with the plates throughout the loading cycle if satisfactory restraint of the wafer is to be accomplished;
c. horizontal in-plane movement of the plates must be restricted while vertical in-plane movement is allowed to facilitate load measurement;
d. the apparatus must accommodate two directional loading (tensile and bending);

e. data must be collected in real-time to enable in-test adjustments to be made.

The complete testing arrangement is shown in Figure 4.2. The design of each of the main components will now be considered.

4.4.1 RESTRAINING PLATE MATERIAL

Plexiglas was chosen as the continuum material because it offered rigidity and machinability. Holes can be cleanly machined in this material with relative ease. The disadvantage of Plexiglas is that it scratches easily. The dimensions of the plates were dictated both by the size of the MTS testing machine and the width of the joint to be simulated. Wafer length was maximized in order to achieve the required bending moment levels with the least amount of lateral force. The edges of the plates were machined for smooth running of horizontal restraining rollers. Holes of 1/2" diameter were drilled through the plates to accommodate the steel pins. A universal joint connected the Plexiglas plates to the load cell via a steel hanger. The final dimensions of each plate was 3/8" X 34" X 5".

4.4.2 ALUMINUM SUPPORTING FRAME

The main purpose of the frame shown in Figure 4.2 was to support the Plexiglas wafer system and to prevent it from moving laterally as the wafer was being loaded.

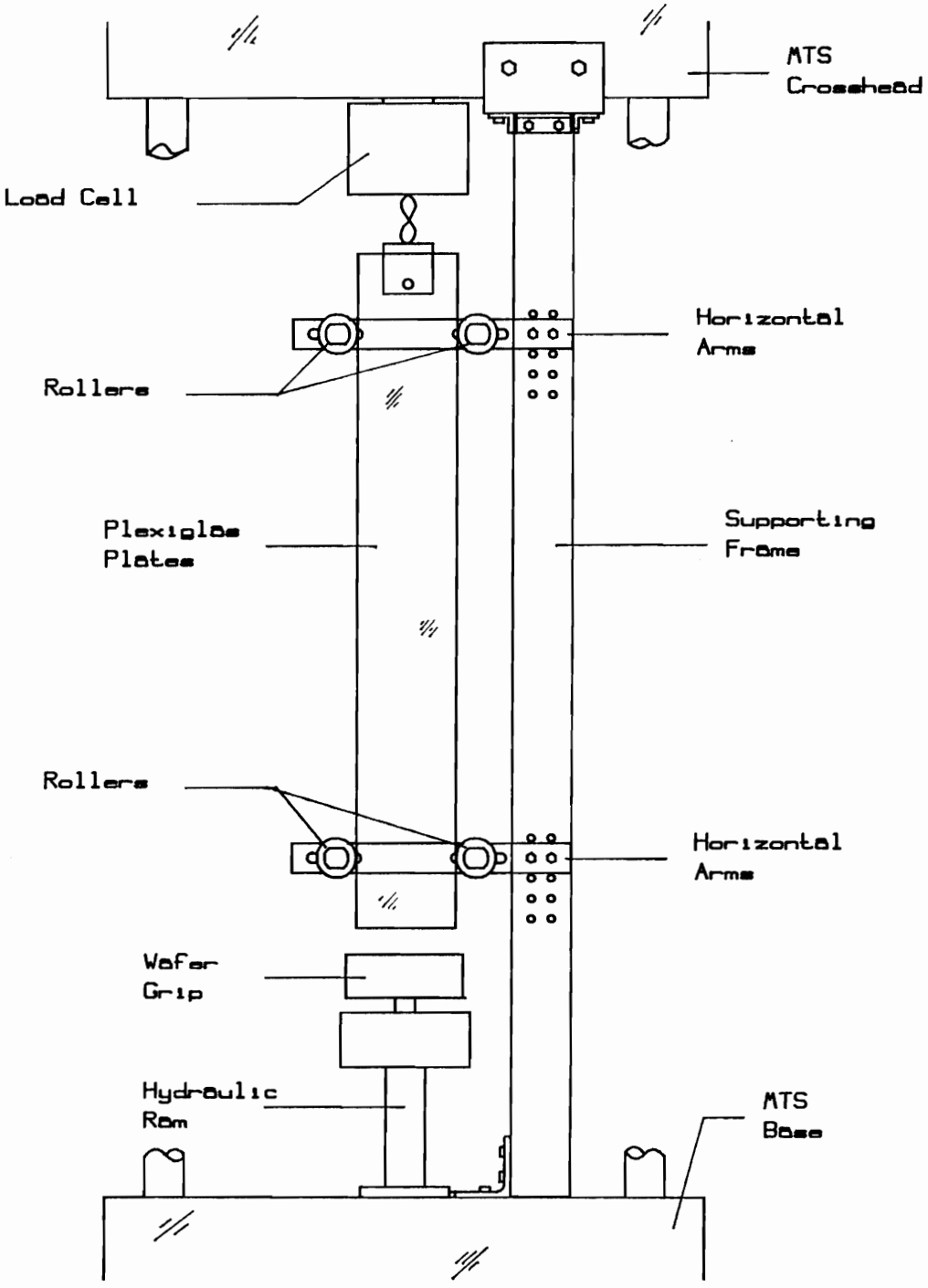

Figure 4.2 Working drawing of the wafer testing apparatus

The bottom of the frame was bolted to the bed of the testing machine, and the top of the frame was mounted onto the static cross-beam. Precision rollers attached to the horizontal arms of the frame formed a low friction track for the Plexiglas plates. This allowed vertically applied loads to be transferred to the load cell. Slots machined into the arms enabled the rollers to be adjusted for accurate alignment of the system (see Figure 4.3). Similarly, the frame was designed to be adjustable when fixed to the testing machine.

4.4.3 AIR GRIPS

A series of hypodermic syringes were used as pistons to clamp the Plexiglas-wafer assembly (see Figure 4.5). These enabled the clamping forces to be accurately regulated independently of small variations in wafer thickness. Thus, it was possible to maintain a relatively constant clamping force from test to test which, in turn reduced the variability in friction.

To achieve uniform clamping the length of the wafer, a total of ten syringes (12 cc capacity) were mounted along the lengths of two thin L-shaped aluminum strips. These were connected to a common regulated air supply. With the syringe plungers retracted, these grips easily slid over the edge of the Plexiglas-wafer sandwich.

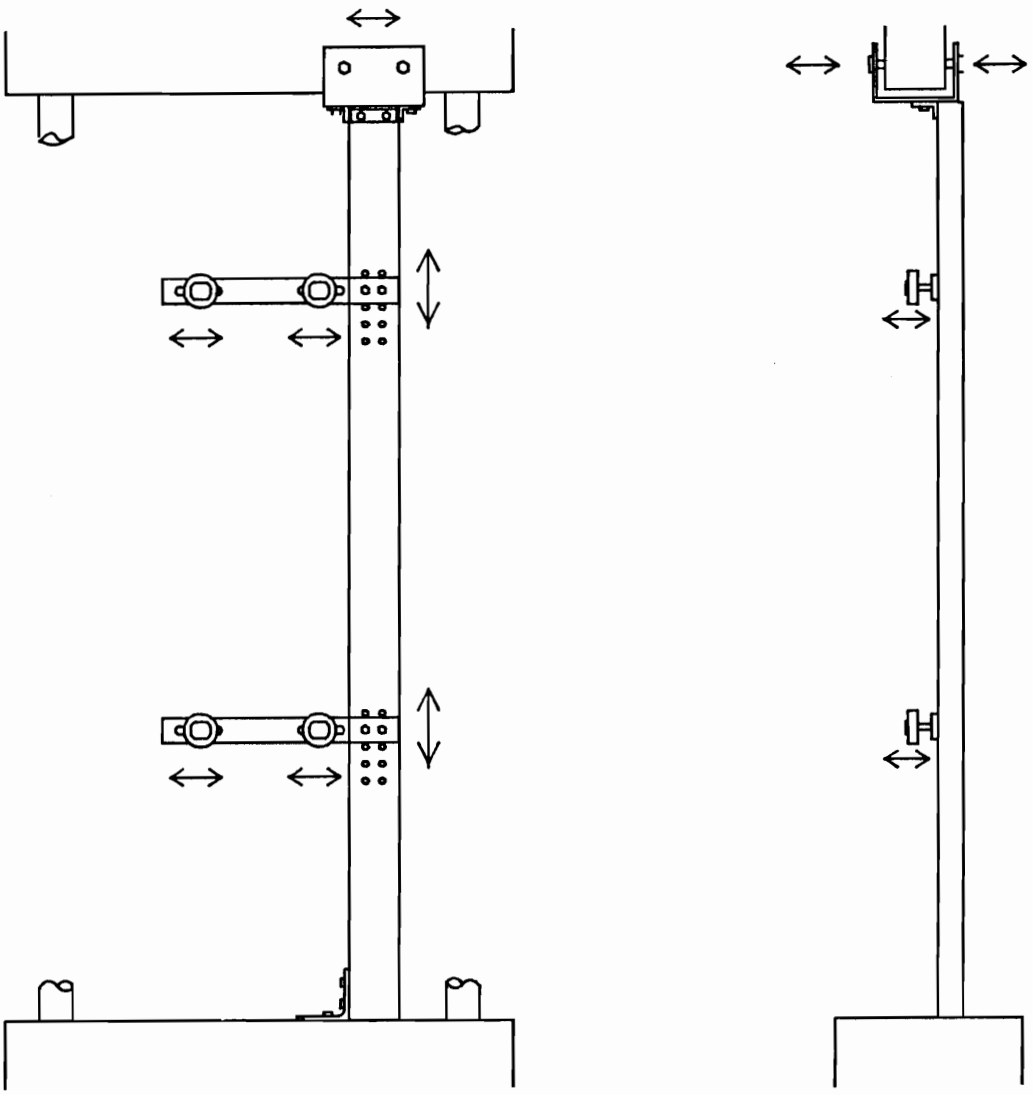

Figure 4.3 The supporting frame showing adjustment points

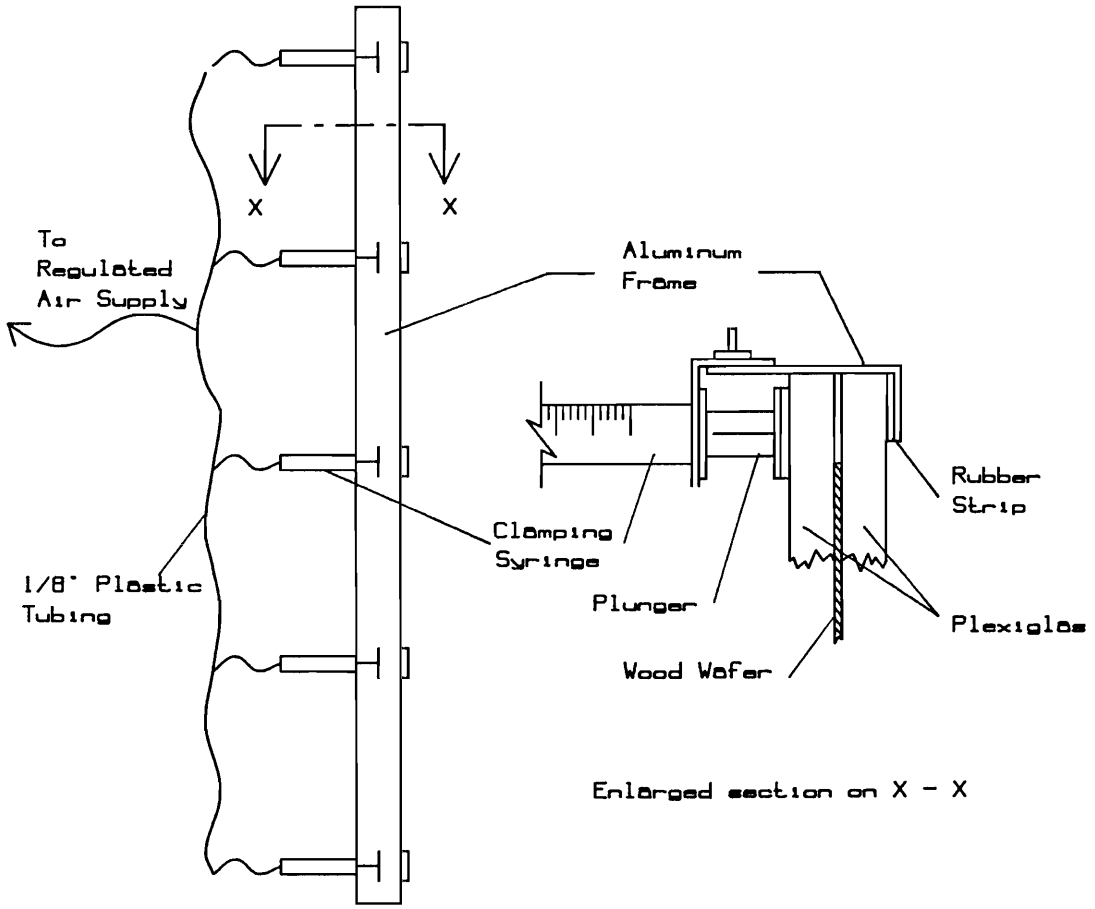

Figure 4.4 Details of the air gripping system

4.4.4 PINS REPRESENTING PORTIONS OF THE BOLTS

Initially, smooth 1/2" diameter stainless steel pins were simply passed through the plate-wafer assembly. It was found in preliminary tests, however, that the crushing of the wood material around the pins tended to force the Plexiglas away from the wafer surface, thus violating the requirement that the surfaces maintain intimate contact.

To avoid this problem, special pins (see Figure 4.5) were designed which held the plates together throughout the

test. Stepped Plexiglas plugs were fitted onto the ends of the pins. Machine screws passed axially through the pin/plug arrangement. By gently tightening the screws, the surfaces were held together.

This method insured intimate contact between the Plexiglas and the wood material where it was most important - around the perimeter of the pin. Unfortunately, localized friction caused by tightening the screws

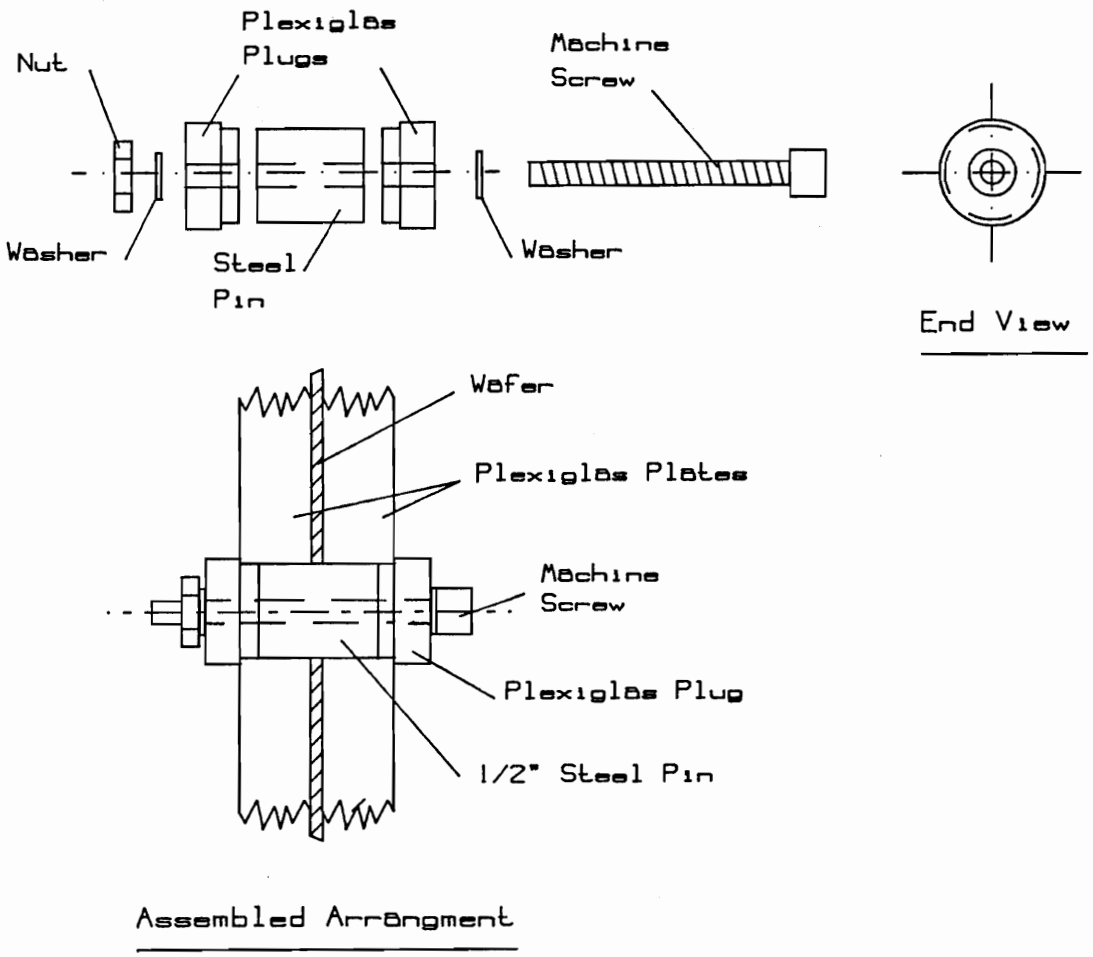

Figure 4.5 Details of the pin assembly

was difficult to control. This drawback partially negated the previously described advantage of using the air grip system. In retrospect a spring loaded assembly may have been more appropriate.

4.4.5 WAFER GRIP AND LOAD APPLICATION ASSEMBLY

Both tensile (axial) and bending (lateral) forces were transmitted to the wafer via a specially designed mechanism mounted on the hydraulic ram of the testing machine. It comprised of a pair of high friction clamping plates connected to a tracking box by a pair of ball bearings. The bearings allowed the grips to slide horizontally in the box. An engineering drawing of the assembly follows as Figure 4.6.

The wafer grip:

The grip consists of five main parts: 1) steel grip plates, 2) set screws, 3) grip stem, 4) ball bearings and 5) LVDT platform. Wafers were inserted between the steel grip plates and the set screws were tightened. To insure even load transfer across the width of the wafer, sandpaper was bonded to the inside surfaces of the plates. The ball bearings mounted at the bottom of the grip stem acted as low friction wheels and ran on specially machined surfaces inside the tracking box. The induction core of the LVDT rested on the horizontal platform.

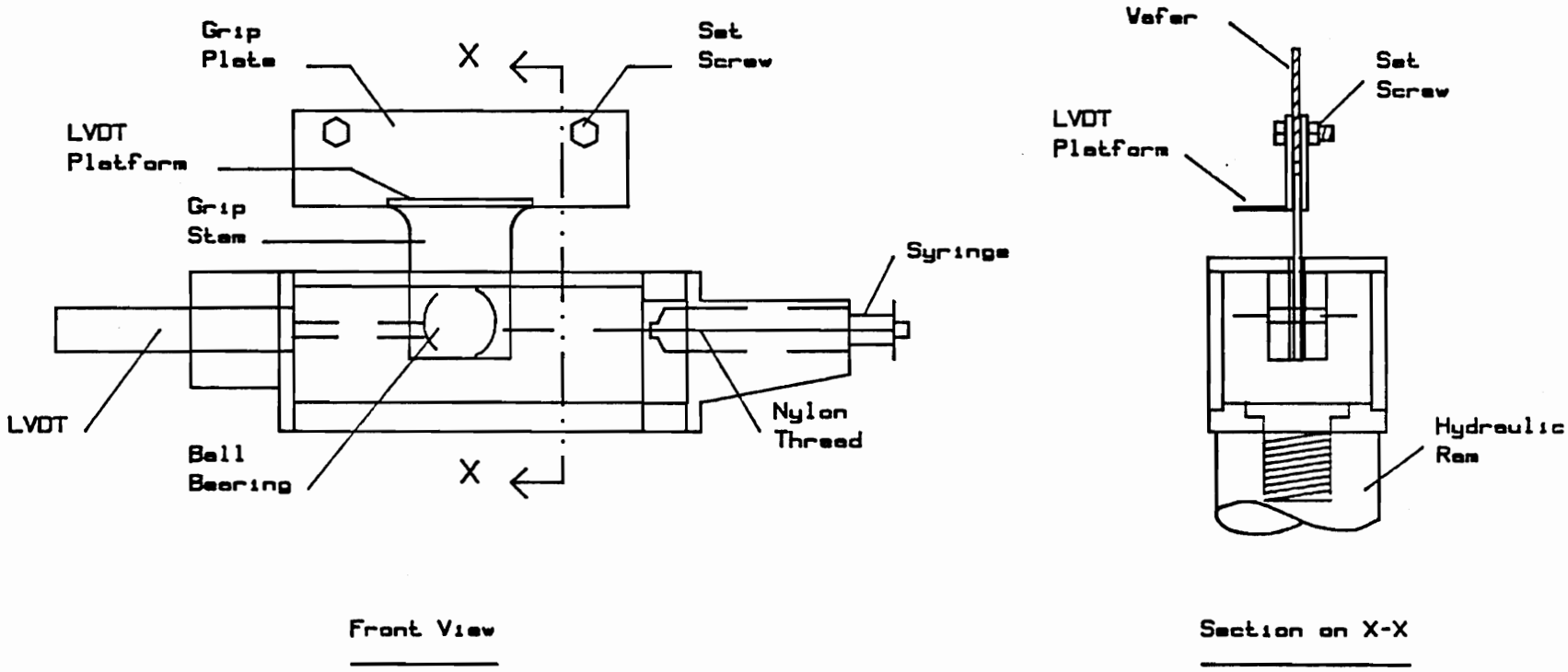

Figure 4.6 The wafer grip and tracking box

The tracking box:

This component linked the hydraulic ram to the wafer grips and guided horizontal movement of the grips associated with joint bending. It also served as a base onto which other pieces of equipment were mounted. A photograph of this arrangement is shown as Figure 4.7 below.

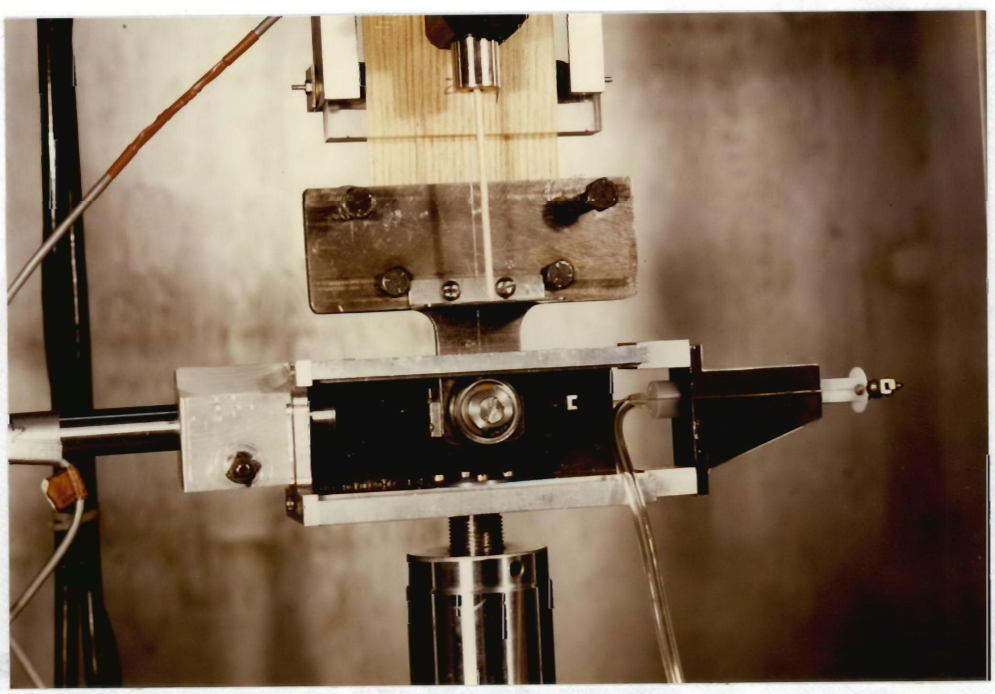

Figure 4.7 A front view of the tracking box, partially disassembled to expose the bearing arrangement

As the grips moved down with the ram, tension was applied to the joint. To apply bending forces, a syringe was mounted on the side of the box. Its plunger was connected to the grip by two high strength nylon threads. Forces were controlled by adjusting pneumatic pressure with

a regulator during each test. Air pressure was electronically measured with a piezoresistive transducer.

Mounting both the syringe and LVDT directly on the tracking box allowed these parts to move together with the wafer. Thus, the horizontal force maintained a constant line of action throughout the test and the measured horizontal displacement was independent of vertical movement of the wafer. This design eliminated several geometrical corrections that would otherwise have been necessary.

4.5 EXPERIMENTAL PROCEDURE

Stages in the testing sequence are listed below.

1. Wafer preparation (refer to section 4.5.1).
2. Wafer alignment (refer to section 4.5.2).
3. Grip alignment (refer to section 4.5.3).
4. Tensile preload applied (refer to section 4.5.4).
5. Scan time, test name, tensile reference voltage entered into data acquisition program.
6. Testing started.
7. Preload released.
8. Horizontal force applied (if required).
9. Tensile force applied.
10. Moment adjusted and monitored (refer to section 4.5.6)
11. Catastrophic failure of the wafer.

12. Data acquisition stops.
13. Photograph wafer if desired.

Vertical friction test (refer to section 4.5.7)

14. Wafer is repositioned.
15. Test information put into data acquisition program.
16. Testing started, tensile force applied.
17. Data acquisition stops.

Horizontal friction test (refer to section 4.5.8)

18. Wafer is repositioned.
19. Test information put into data acquisition program.
20. Testing started, horizontal force applied.
21. Data acquisition stops.

4.5.1 ASSEMBLING THE TEST

At the start of each test, a wafer was placed between the two sheets of Plexiglas and the pin assembly was inserted into the holes. The screws of the pin assembly were hand tightened sufficiently to bring both surfaces of the Plexiglas in contact with the wafer. Further tightening of the screws was avoided because of the very high frictional forces that resulted. After the pins were tightened, the assembly was mounted onto the universal testing machine.

4.5.2 WAFER ALIGNMENT

The slightly oversized holes caused small cracks of light to appear wherever there was a gap between the pins and the wafers. The wafer holes were centered about the pins using these gaps as guidelines. When in this position, the wafer was regarded as being "in-line" and the test could be started.

4.5.3 GRIP ALIGNMENT

Because forces were applied through the grip, it was very important that the grip be properly positioned before it was connected to the wafer. The grip was centered on the wafer so that if a line were drawn vertically through the central axis of the pin configuration, it would intersect the grip at its midpoint. This insured that the line of action of the vertical force was directed through the center of the wafer. In addition, the distance between the grip and the top edge of the wafer was kept constant for each test to reduce the number of variables in the moment calculation.

4.5.4 INITIALIZATION OF THE DATA COLLECTION SYSTEM

To start each test in a zero load condition, the grip had to hang freely without contacting the tracking surface. During the first moments of tensile loading, the LVDT measuring vertical displacements would produce erratic

voltage readings as the bearings from the grip aligned themselves with the tracking box.

In order to avoid recording this initial grip alignment as actual slip of the joint, each test was started when the wafer had a very small preload applied, enough to bring both bearings into contact with the track. In order to avoid using this preload value as the zero reference voltage for tensile load, the true zero reference voltage was input to the program prior each test.

4.5.5 DATA SHEETS

Along with the hard copy of disk written data and the load-slip curves supplied by an x-y recorder, certain data were manually recorded to keep a record of each test. Data sheets included observations of the test, a drawing of the failure characteristics, and any other observations made during the test. Also recorded were testing speed, grain direction and important voltage readings. These sheets served as a general reference guide when analyzing the data and helped to organize the test procedure.

4.5.6 MONITORING THE MOMENT APPLIED TO THE JOINT

The bending moment for the system can be calculated as follows (refer to Figure 4.8):

$$M = F * d \qquad (4.1)$$

where d = distance from the centroid of the configuration to the point of application of force F.

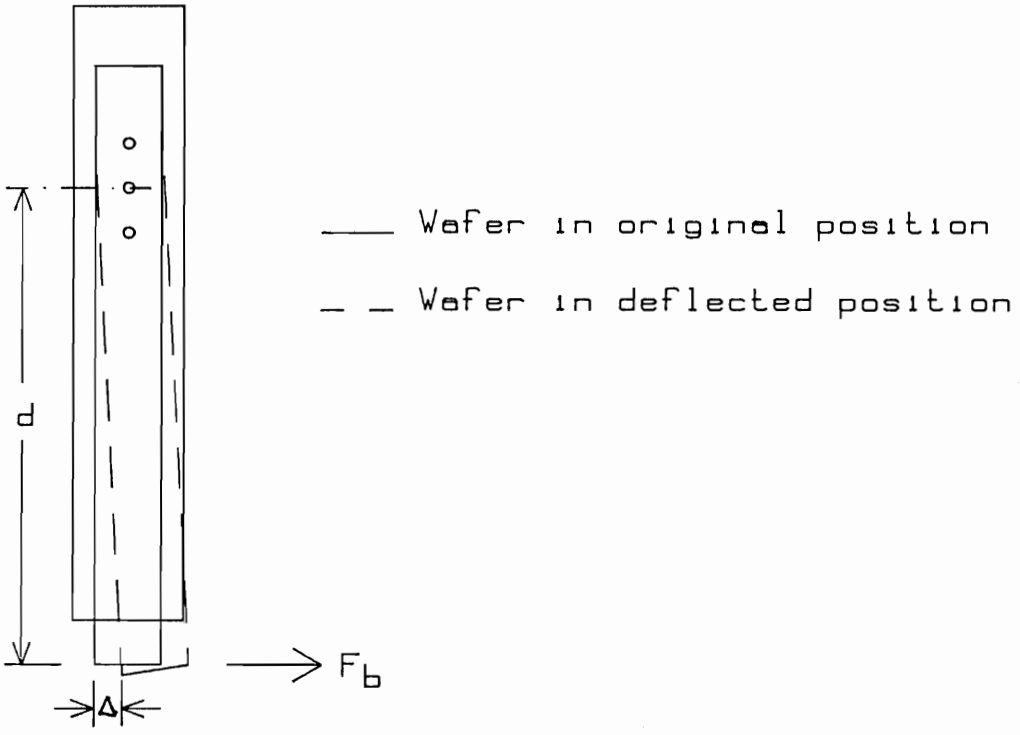

Figure 4.8 The wafer under combined loading showing resulting lateral displacement

It will be assumed that under horizontal (bending) forces, the wafer will tend to rotate about the centroid of the geometrical configuration. Wood material adjacent to the sides of the pins is compressed as the wafer is displaced horizontally by an amount delta,(Δ). This displacement depends on the magnitude of the horizontal force, bolt geometry, wood stiffness (affected by wood damage) and distance d.

Horizontal loads (bending moments) were applied prior to the progressive application of tensile loads to failure. As the tensile load was increased, an opposing moment equal to $T * \Delta$ was created. The total moment on the joint can be calculated as:

$$M = (F * d) - (T * \Delta) \qquad (4.2)$$

Thus, increasing T without changing the other factors in the equation results in a progressive reduction of the moment and it follows that F must be increased in order to maintain a constant moment on the joint.

The initial moment is given by:

$$M_{initial} = F_{initial} * d \qquad (4.1)$$

After a tensile load is applied, the moment on the joint is given by:

$$M_{new} = (F_{initial} * d) - (T * \Delta) \qquad (4.2)$$

The additional force required to maintain the moment is:

$$F_{additional} * d = T * \Delta \qquad (4.3)$$

rearranging leads to:

$$F_{additional} = \frac{T * \Delta}{d} \qquad (4.4)$$

Substituting into equation (4.2) gives:

$$M_{new} = (F_{initial} + F_{additional}) * d - (T * \Delta)$$

The bending moment on the joint was repeatedly calculated by the computer and displayed on the screen as the test progressed. If this value deviated from the original target moment value, the horizontal force was manually adjusted. Figure 4.9 shows a typical moment vs. time curve for one of the tests. Small variations in moment occurred because crack propagation in the wafer caused sudden increases in the horizontal displacement. This rapid increase in horizontal displacement required considerable changes in the magnitude of the horizontal force and these could not be affected instantaneously.

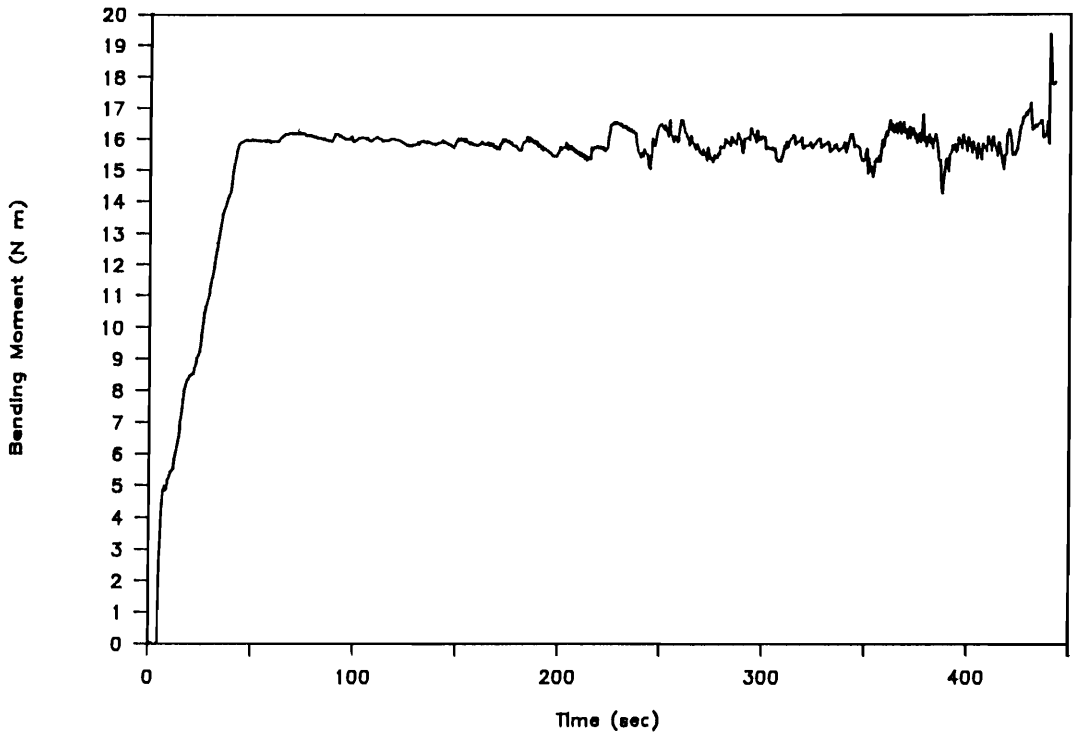

Figure 4.9 A moment versus time curve for a typical test

4.5.7 VERTICAL FRICTION TESTS

Following joint failure, frictional calibration tests were performed. The process of loading the wafer to failure resulted in a crushing of the wood material surrounding the hole. This crushing created elongated holes. Without removing the grips or altering the system in any way, the wafers could be moved back into their original position leaving gaps above each hole. This allowed the wafer to slide freely for a limited distance before the wood material contacted the pins. By applying tensile forces to the wafer, load-time curves were generated and used to derive the vertical friction forces.

4.5.8 HORIZONTAL FRICTION TESTS

After catastrophic failure of the joint occurred, large cracks extended through the wafer. These cracks, allowed the wafer to slide freely in the horizontal direction for a limited time without encountering much resistance. Horizontal frictional forces could be derived by measuring the force required to initiate such lateral sliding.

4.6 DATA ACQUISITION DURING WAFER TESTING

Each of the variables required to characterize the joint during testing will be considered. This will be followed by a description of the computer program used for data acquisition.

4.6.1 LOAD AND DISPLACEMENT MEASUREMENTS

Measurement of tensile loads:

To measure tensile load, a three hundred pound capacity load cell was mounted onto the cross beam of the MTS. The load cell was calibrated and a zero offset was measured but sensitivity remained linear.

Measurement of vertical displacement:

To monitor actual vertical displacement of the wafer, the LVDT was mounted to one of the Plexiglas plates while the induction core rested on a steel platform fastened to the grip below. Thus, wafer movement relative to the pins

was measured. An LVDT with a range of 0.1" was used for this measurement since axial slips of the joints prior to failure were small.

Measurement of horizontal displacement and load:

To simplify the moment calculations, the body of the LVDT measuring horizontal displacement was mounted directly onto the tacking box and the induction core was attached to the grip so that it was in line with the point of application of lateral force. Horizontal movement of the wafer was substantial and required the use of an LVDT with a 0.5" range.

Applied lateral forces were calculated using the output of the pressure transducer (0 - 30 psi range) used to measure the air pressure driving the piston.

4.6.2 THE DATA ACQUISITION PROGRAM

Tensile load, horizontal load, vertical displacement and horizontal displacement were recorded using a microcomputer equipped with an eight channel analog to digital conversion board (No. DT 5205 A, manufactured by Data Translation Inc.). DC voltages from each measuring device were directed to the board via a specially manufactured interface unit (one channel per device). The voltages from each device were translated into scientific units using conversion factors specific to each device.

Every 0.16 seconds, the board recorded data from one

channel. Channels were scanned in sequence, therefor each channel was scanned every 0.64 seconds. Voltage values were stored in an array after analog to digital conversion.

During the first scanning sequence and before any testing loads were applied, output voltages from each device were established as zero references. As a test progressed, subsequent changes in pressure, load and displacement were measured relative to these voltages. In this way, linear sensitivity could be applied directly when converting the raw data into scientific units (ie; zero offsets were avoided).

With each successive scan of the four channel series, the instantaneous bending moment on the joint was calculated and compared to the target moment set at the beginning of each test. The current moment and any difference between it and the target moment were displayed on the screen. Adjustments in the lateral force were made manually by changing the pressure acting on the piston in order to bring the two values into agreement.

Other recording devices:

To supplement the primary data recorded with the computer, an X-Y recorder was used to monitor tensile load as a function of time. These load-time graphs gave a real-time indication of how the system was performing while a test was in progress. They were also compared to the load-slip curves derived from the computer collected data to

check for discrepancies.

In addition, a number of wafers were photographed after they had failed. These were used to compare the types of failures that resulted when a particular configuration and bending moment were tested.

4.7 DATA REDUCTION

Data reduction involved two distinct phases. Analog to digital conversions (section 4.6.2) were performed by the computer in "real time" before data were stored on the disks. Secondary geometrical and frictional corrections were carried out after testing was complete. These secondary adjustments are discussed in this section.

4.7.1 CORRECTING TENSILE LOAD VALUES FOR FRICTION

Load-slip curves obtained during friction tests provided the information necessary to calculate the tensile static frictional force, μ_t. Figure 4.10 shows a typical friction curve for one of the tests. Peaks on the curve, representing the static frictional force of the system when the wafer was loaded in the vertical direction, were matched with the corresponding values stored in the data file. Values for μ_t were calculated by taking the average of these values. Any peak which had a value within 5 Newtons of the first peak's value was included in the average. With this, an tensile vertical frictional force for each wafer was derived.

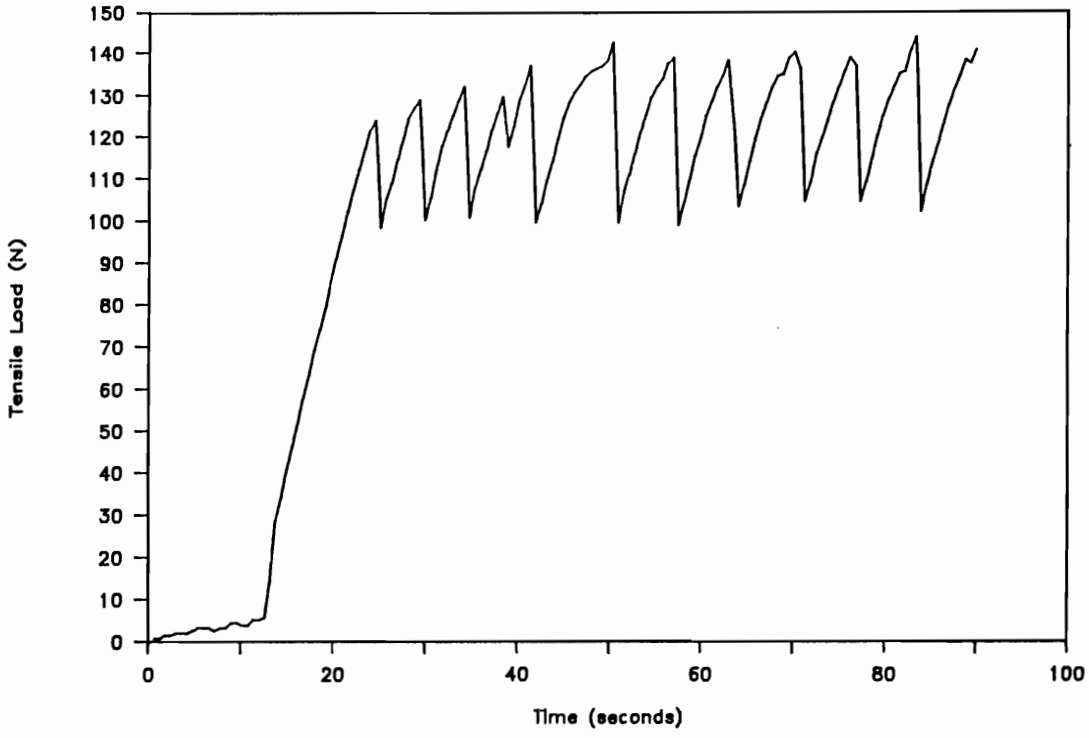

Figure 4.10 Tensile load versus time curve used to derive tensile frictional forces, μ_t

Actual tensile load values transferred from the wafer to the pin were determined by subtracting the derived μ_t from the measured tensile forces.

4.7.2 DEFINING THE STARTING POINT OF EACH TEST

To simplify the analysis, the starting point of each test was defined as the time during the loading cycle when the corrected tensile load equaled zero. This is referred to as the test initialization time, t_i. All corrections and derived values discussed in the remainder of this chapter are based on taking t_i as a starting point.

4.7.3 DERIVATION OF ANGULAR DISPLACEMENT VALUES, θ

Figure 4.11 shows a deflected wafer after a horizontal load has been applied. The angle formed between the deflected wafer and the vertical axis, θ, was derived using equation 4.5.

$$\theta = \frac{\tan^{-1} \Delta x}{d} = \frac{\Delta x}{783.18 \text{ mm}} \qquad (4.5)$$

where: x = horizontal displacement of the wafer recorded by the LVDT at time t_i.

d = distance from the center of the bolt configuration to the LVDT

4.7.4 CORRECTING TENSION FOR ANGULAR DISPLACEMENT (θ)

F_{axial}, the load which acts along the main axis of the wafer in Figure 4.11, may be derived from its horizontal and vertical components as follows:

$$F_{axial} = (F_t * \cos\theta) + (F_b * \sin\theta) \qquad (4.6)$$

F_b and $\sin\theta$ were negligible compared to F_t and $\cos\theta$. This leaves

$$F_{axial} = F_t * \cos\theta \qquad (4.7)$$

which represents the axial tension in the wafer.

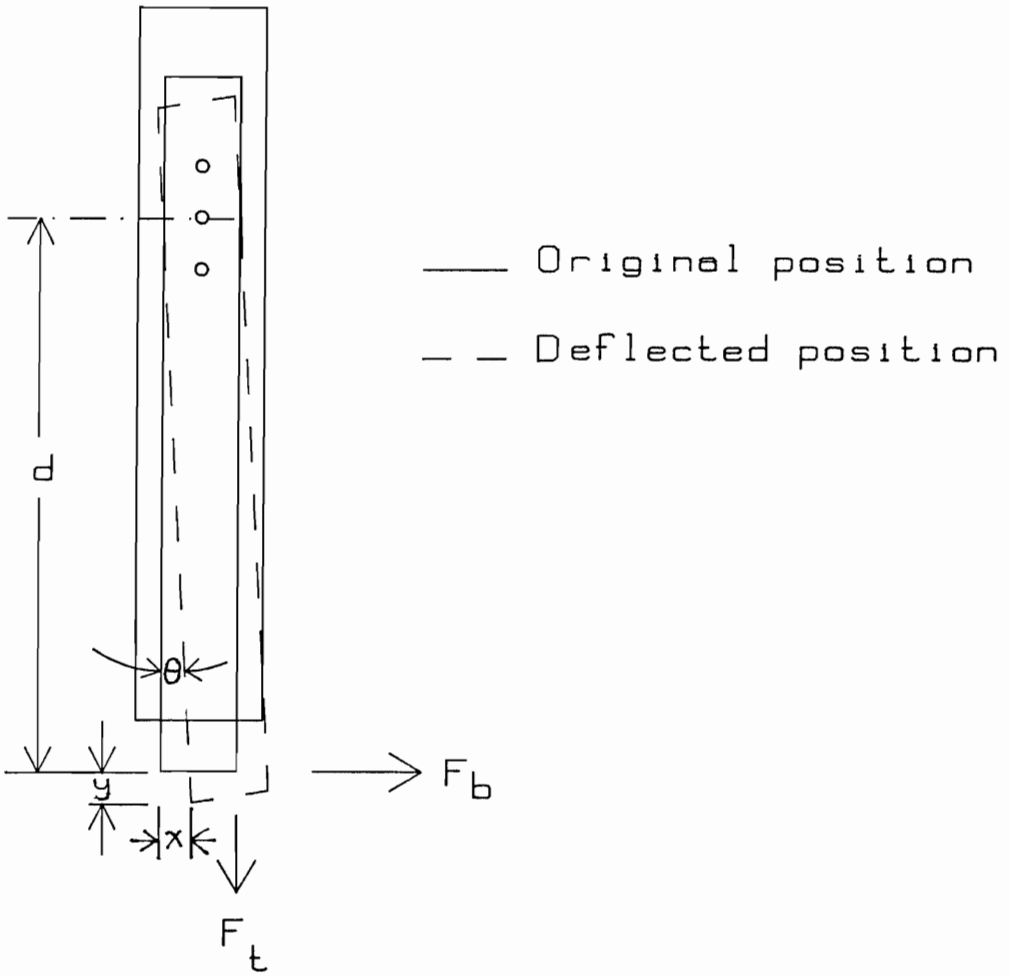

Figure 4.11 A wafer under combined loading showing resultant angular and longitudinal displacements

4.7.5 CORRECTING VERTICAL SLIP VALUES FOR CHANGES IN MEASURING GEOMETRY

In section 4.4.6, the wafer grip and LVDT platform were described. Figure 4.12 shows the platform geometry after the wafer is displaced horizontally. The changing angle of the platform distorts measured vertical displacement values and requires geometrical corrections to be

made. The angles used in Figure 4.12 have been exaggerated to show the corrections more clearly. Equation 4.8 has been derived to correct for the platform error.

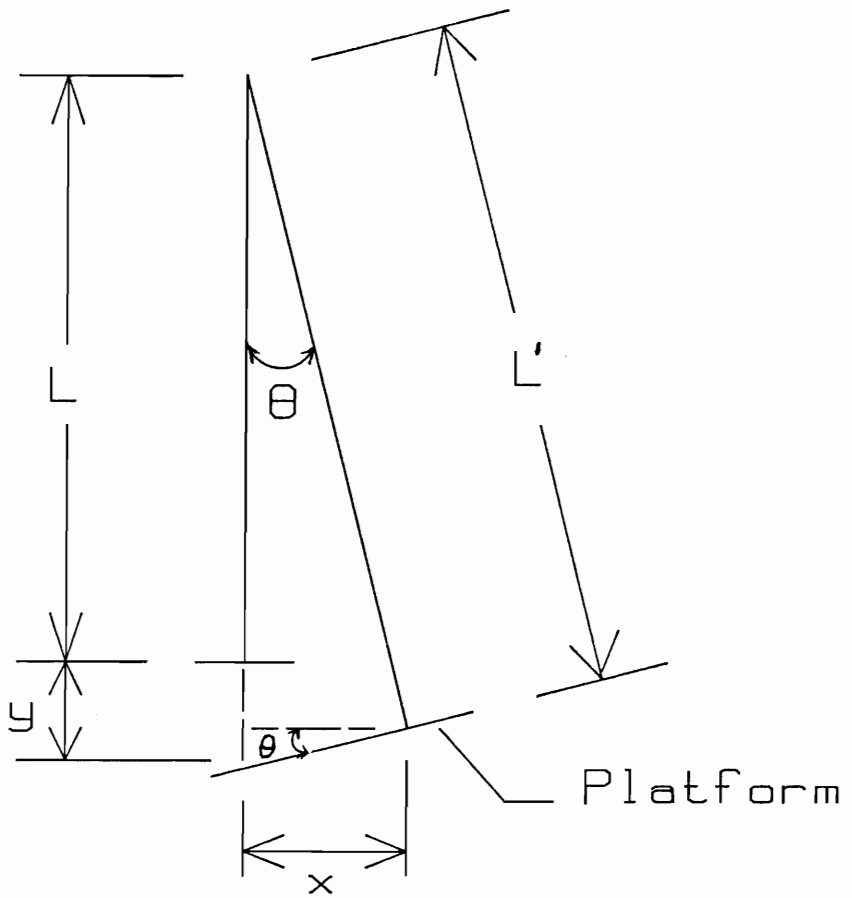

Where L = initial distance from centroid of pin configuration to platform ≈ 783mm

L'= distance from centroid of pin configuration to platform after displacement

y = uncorrected vertical displacement

x = horizontal displacement

Figure 4.12 Geometrical corrections of the deflected wafer and platform

$$L' = \frac{L + y - x * \tan\theta}{\cos\theta} \tag{4.8}$$

$$L = L' - L \tag{4.9}$$

$$L = \frac{L + y - x * \tan\theta}{\cos\theta} - L \tag{4.10}$$

After this correction, the slip value at time t_i should equal zero. Small inconsistencies that remained were made good by shifting the load-slip curve slightly.

4.7.6 CORRECTING MEASURED BENDING FORCES FOR FRICTION

Curves used to derive bending frictional forces, μ_b, (see Figure 4.13) did not exhibit the saw-toothed form of their vertical counterparts and therefor did not lend themselves to the same type of analysis. Bending friction curves were developed using load-control whereas the vertical ones were developed under position-control.

The bending force which caused 4 mm of horizontal displacement was defined as μ_b . This displacement value was selected in light of certain slack tolerances in the system which limited the reliability of load measurements made a values lower than 4 mm.

These values remained relatively constant for each test. Consequently, the μ_b values for each test were averaged for each of the three series. The corrected horizontal load was calculated by subtracting the derived frictional values from measured horizontal forces.

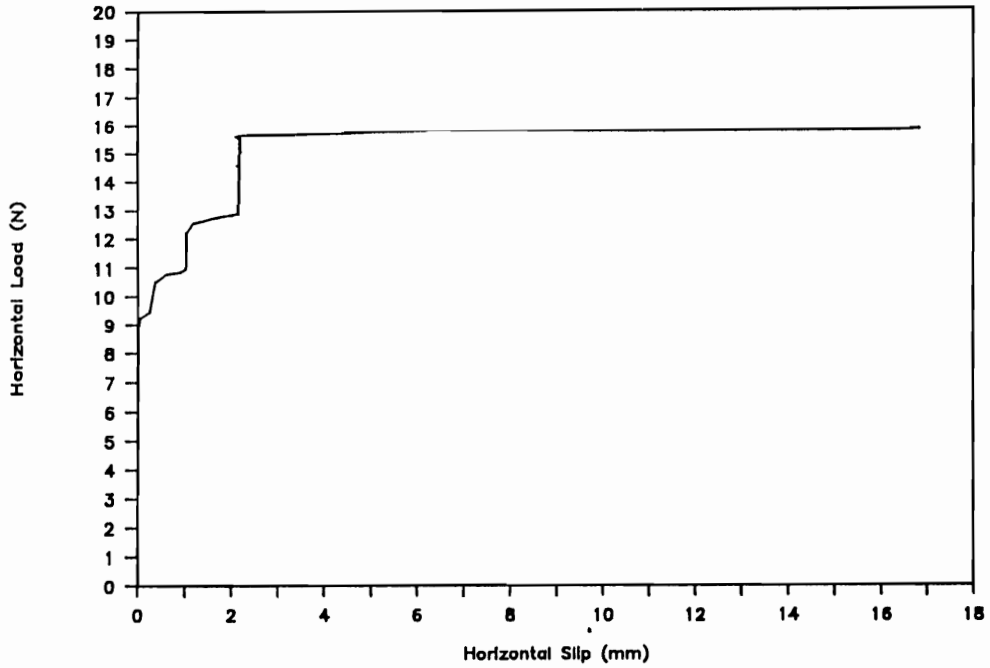

Figure 4.13 Typical load versus slip curve used to derive bending frictional forces, μ_b

4.7.7 CURVE PLOTTING

Tensile load versus vertical slip curves were plotted for each test. Averaged curves are presented in chapter VI.

Changes in the bending stiffness of the wafer joints as they were loaded were observed for a selected number of test by plotting horizontal deflection against applied tensile load. It is worthwhile to note that these curves do not necessarily go through the origin because horizontal loads were applied first, causing horizontal deflection (theta) to develop before any tensile loads were applied.

It was hoped that these curves would reflect the change in bending stiffness of the joint. As a joint is

loaded in tension, the wood material is damaged and the resistance to bending is decreased. Thus, with appropriate force control, horizontal deflection should increase with increases in tension. This effect reflects the weakened nature of the joint.

Tests were divided into categories according to the particular joint configuration ("L-R", "V-R" and "L-T") and bending moment level being tested. At least two replications were performed for each joint configuration/bending moment combination. The load-slip data for all replications of a given test combination was averaged. Digitizing of each curve was necessary prior to averaging since there was no consistency in increments for either variable. Averaging enabled a single load-slip curve to be produced for each joint configuration/bending moment combination.

Following the averaging procedure, the standard deviation of the load values at each slip was calculated. With this statistic, confidence intervals could be plotted, if desired.

Because ultimate failure point varied for each wafer, the length of the load slip curves being averaged varied. To accomodate this, the shortest curve within the group, that which had the smallest slip at time of failure, was identified. Only points which were less than or equal to this minimum slip value were used when averaging the other curves. Points lying beyond this minimum slip value were ignored.

Some curves exhibited negative displacement at the early stages of loading. This most likely was due to misalignment of the wafer grip. This phenomenon was accounted for by redefining the origin in the digitizing process (see Figure 4.14).

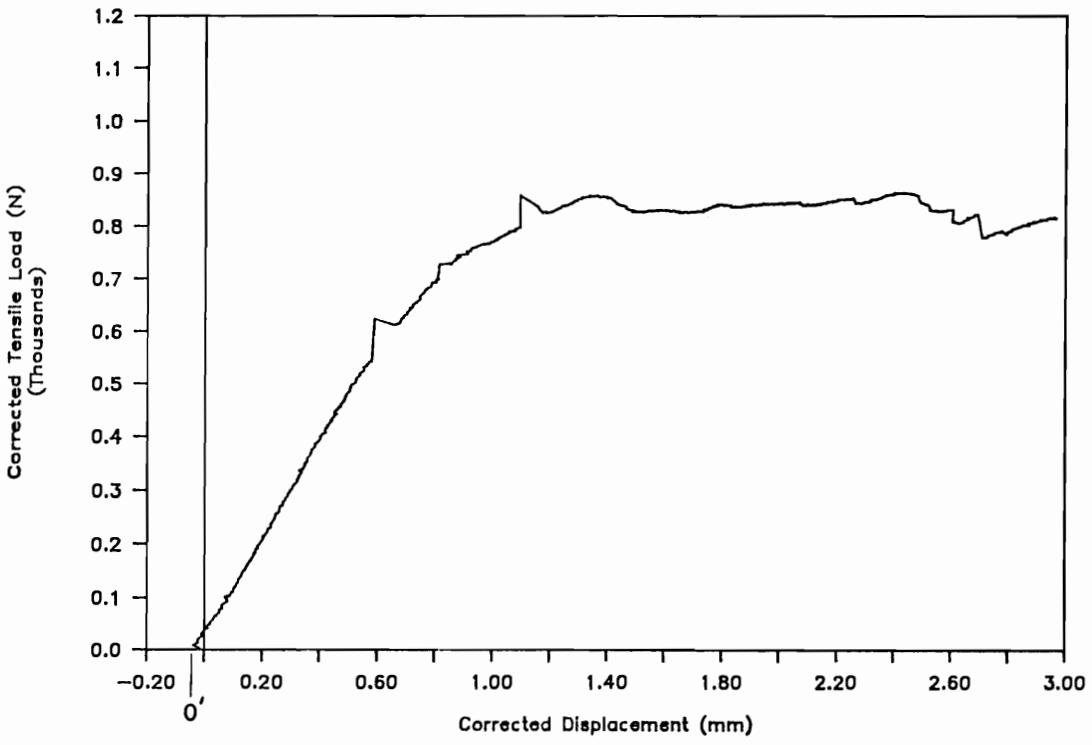

Figure 4.14 Tensile load versus slip curve showing peaks caused by electrical noise, and negative displacement values with redefined origin O'

Sudden apparent periodic load increases occurred during some tests. These jumps, shown in Figure 4.14, may have been caused by electrical noise received by the testing machine through the power supply. This irregularity was corrected for by connecting the two discontinuous points with a smooth line prior to digitizing.

A discussion of all graphs mentioned in this section will appear in chapter IV.

Chapter V

TESTING OF WHOLE JOINTS

5.0 INTRODUCTION

A limited number of complete joints were subjected to a series of combined tensile and bending forces. This portion of the study, carried out with the help of Research Assistant Ken Bastendorff, was a preliminary investigation used to verify the results obtained from the wafer approach. The chapter outlines the main aspects of these preliminary full scale tests.

5.1 MATERIAL SELECTION AND JOINT MANUFACTURE

The joint design used in these tests was presented as Figure 3.2 and used as the basis for the wafer method. It consists of a wooden main member and two wooden side members connected by three 1/2" diameter bolts in a single row. Bolts were spaced according to specifications outlined in the 1982 edition of the NFPA National Design Specifications (15). Lack of materials and time prevented the testing of any other configurations at this time.

A preliminary investigation of the effects of lumber grade on joint performance under combined loading was also conducted. Two lumber grade classifications were used in the construction of the members. Unfortunately, only the side members were of MSR material; the grade of lumber used

in the main members was not accurately known. This may reduce the significance of this part of the study.

The side members were made from 2" x 4" (nominal) MSR Douglas-fir lumber purchased from Frank Lumber Company, Mill City, Oregon. The high grade lumber had assigned bending strength values between 2100 psi and 2400 psi, and a modulus of elasticity of approximately 1.9 X 10^6 psi. Low grade material had bending strength values of 1300 psi and an MOE of 1.3 X 10^6 psi.

Main members were manufactured from a 5" x 24" x 24' glue-laminated beam kindly donated by Weyerhauser, Inc. in Cottage Grove, Oregon. Glulam was used because it was available kiln-dried in large dimensions. This minimized the potential for drying defects such as checking and dimensional change.

To construct each member, the beam was cut into sections 4' in length. Because the wood material used in the outermost laminations of a glulam beam is stronger than the material in the interior portions, each 4' long section was divided into two strength classes. Higher strength material consisted of the first three exterior laminations, while lower strength material made up the inner portion of the beam.

Figure 5.1 shows the cutting pattern used to manufacture main members. By using this pattern, glue lines were always located at the same position in each piece. Surfaces were free from glue and were planed to

control the surface frictional coefficients. This pattern also ensured that the bolts would not pass through a glue line. Work done using glue lines oriented perpendicular to the bolt axis has been a concern of some researchers in the past.

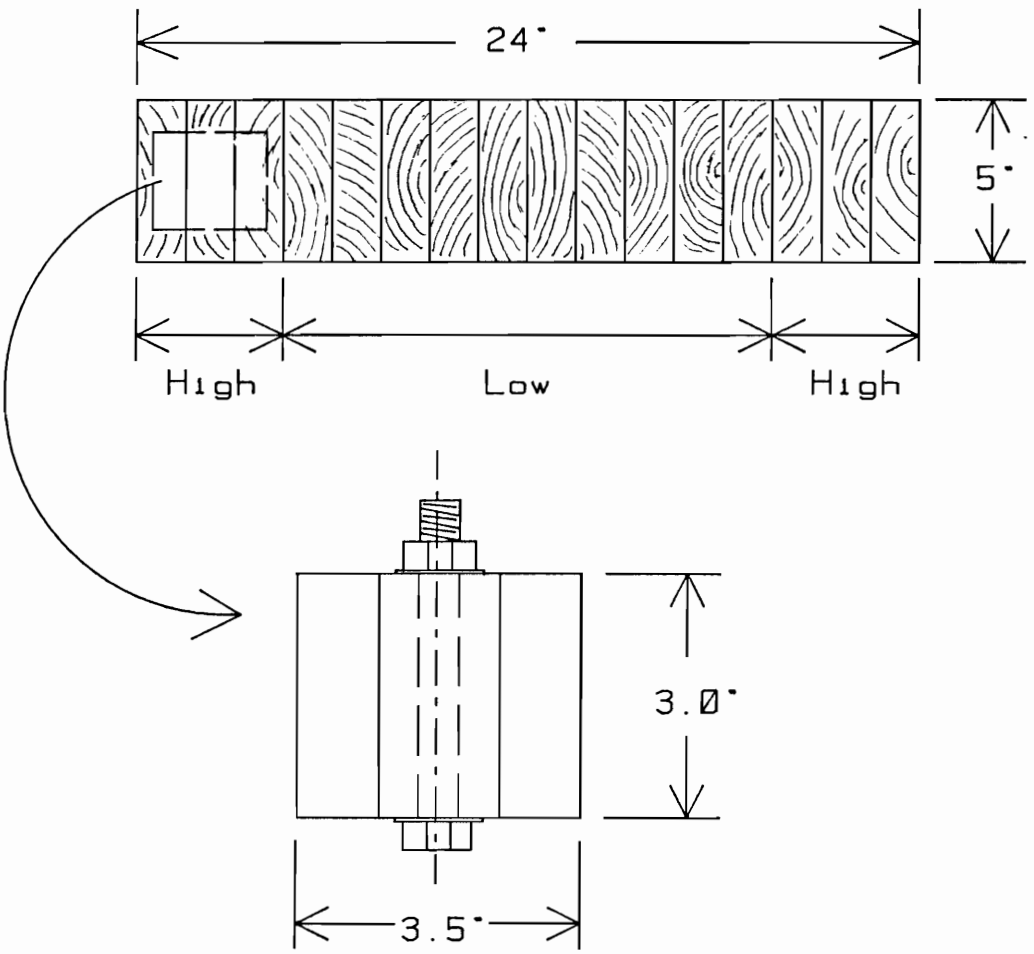

Figure 5.1 Transverse cross section through the glue-lam beam showing strength differentiation of material and orientation of bolt though main members.

Once the members were machined to their final dimensions, main members were matched with side members of the corresponding strength grouping. The three members were drilled simultaneously using a jig on the drill press. Bolts usually required some tapping with a mallet to seat them properly. Washers were used at both ends of the bolt and the nuts were turned until finger tight. A typical finished joint is shown in Figure 5.2. The bolts have been partially exposed for illustration purposes.

Figure 5.2 A typical full scale joint

5.2 BENDING MOMENT LEVELS

As with the wafer technique, both bending and tensile forces were simultaneously applied to most of the joints.

Preliminary testing of twelve joints helped to determine upper and lower strength limits for the range of loading modes to be investigated. Three joints of mixed lumber were tested in pure bending to determine the maximum bending strength of a typical joint. These joints yielded at 1408 lbs., 1678 lbs. and 1714 lbs. In addition, three joints made from lower strength material were tested in pure tension and six were tested under combined tensile and bending forces.

The results of these tests were used to select the four different bending moment levels which would be applied to the joints. The bending moment values employed are shown as Table 5.1.

Table 5.1 Bending moments used to test full scale joints

Bending moment (N·m)	Replications	
	Higher strength material	Lower strength material
0	3	4
595	2	4
857	5	4
1143	1	0
1236	1	0

5.3 TESTING APPARATUS DESIGN

The main functions of the apparatus used for whole joint testing were:

1. To simultaneously apply bending and tensile forces to the joint.
2. To apply a constant moment across the bolted portion of the joint.
3. To allow the bending force to be adjusted during the test.

Additional functions of the specially designed steel frame were as follows:

a. To transfer tensile forces from the testing machine to the members;
b. To support the load bearing blocks that supplied the lateral bending force;
c. To house the load cell and hydraulic cylinder.

The arrangement is shown diagramatically as Figure 5.3.

The members were supported by steel tension bars which were pinned to the universal testing machine. Tension was applied to the joints through the crosshead which moved at a rate of 1.2 mm/minute. This was approximately twice as fast as the rate used in the wafer approach.

The two radiused load bearing blocks were pivot connected to a load evener as specified by ASTM D198 (1). The 10" separation between these blocks was sufficient to

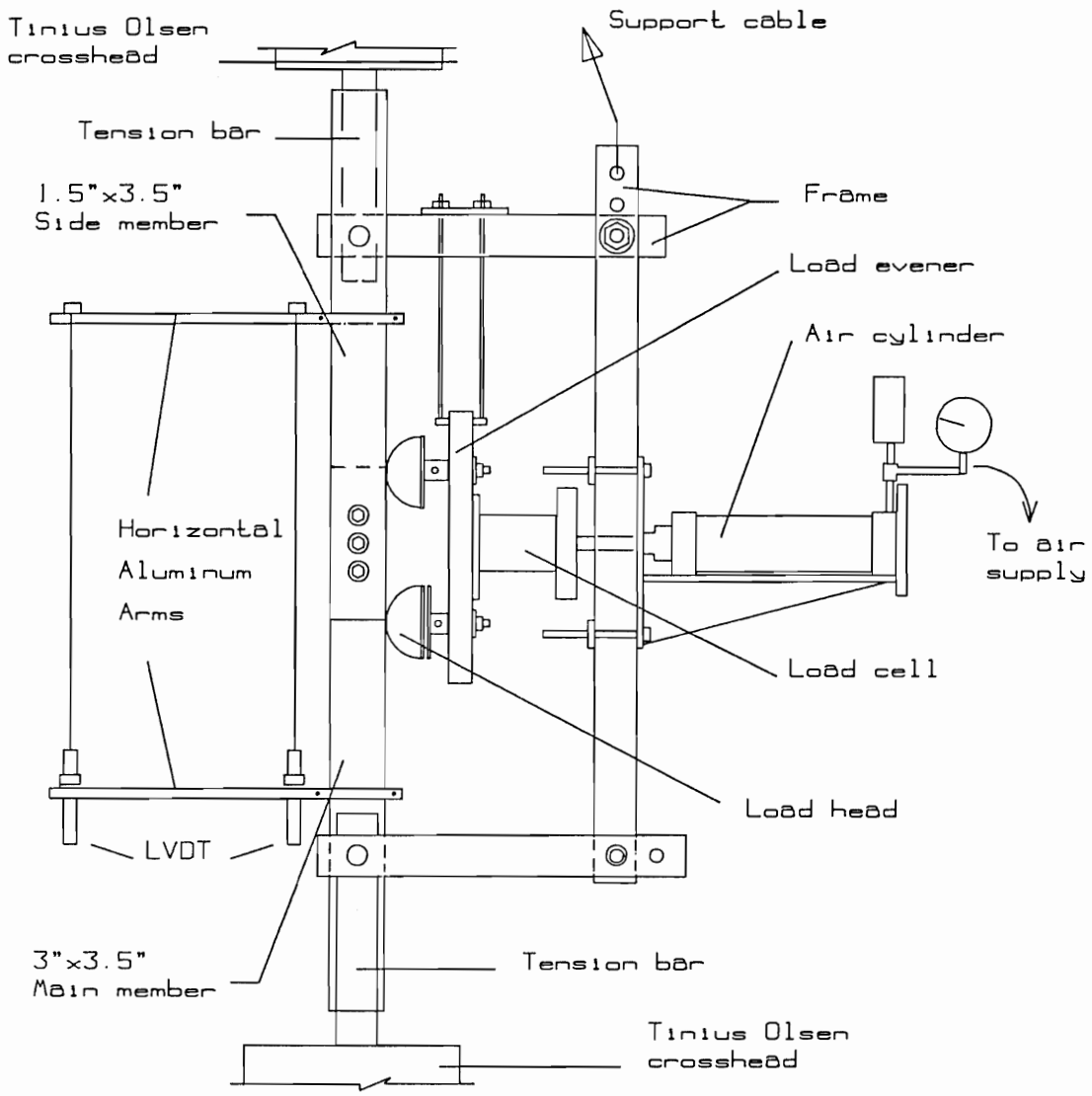

Figure 5.3 The testing apparatus used with whole joint testing

span the bolted portion of the joint. A 3 1/2" diameter hydraulic cylinder was used to supply the bending force. The cylinder was driven manually with a hand pump which supplied fluid to the cylinder in a controllable manner. To measure the bending force, a 300 pound capacity load cell was connected in line between the load evener and cylinder.

To measure both joint rotation and elongation, two aluminum arms were independently clamped to the members. This will be discussed in section 5.5.2.

5.4 EXPERIMENTAL PROCEDURE

This section summarizes the steps taken during the testing of one joint.

Prior to the start of the test:

1) The joint is assembled and mounted in frame.
2) A small tensile preload is applied to the members to straighten out any misalignments.
3) Preload is released.
4) Scan time, test name, and target bending force are entered into the computer program.
5) Final check of assembly.

After testing begins:

6) Data acquisition program is started.
7) Target bending force is applied (if required).
8) Tensile force is applied (cross-head movement is initiated).

9) Bending moment is monitored and bending force is adjusted as necessary (refer to section 5.4.1).

After catastrophic failure:

10) Data acquisition stops.

11) Results are graphed.

12) Testing complete.

5.4.1 MONITORING THE MOMENT APPLIED TO THE JOINT

Bending moments were produced in the joints by applying a horizontal force to the members through a two point loading system added to the tensile loading frame on the testing machine. This approach produces a uniform bending moment between the load bearing blocks. Using the free body diagram shown as Figure 5.4, the moment acting on the joint (between the load bearing blocks) can be calculated as:

$$M = \frac{F}{2} * x \qquad (5.1)$$

The simultaneous application of the tensile and lateral forces causes the joint to both elongate and bend. The straightening moment produced by the tensile force acting through the laterally deflected joint tends to oppose the moment produced by the applied lateral force. Thus, as the product of tensile force and horizontal displacement (Δ) increases, the true moment within the joint tends to decrease.

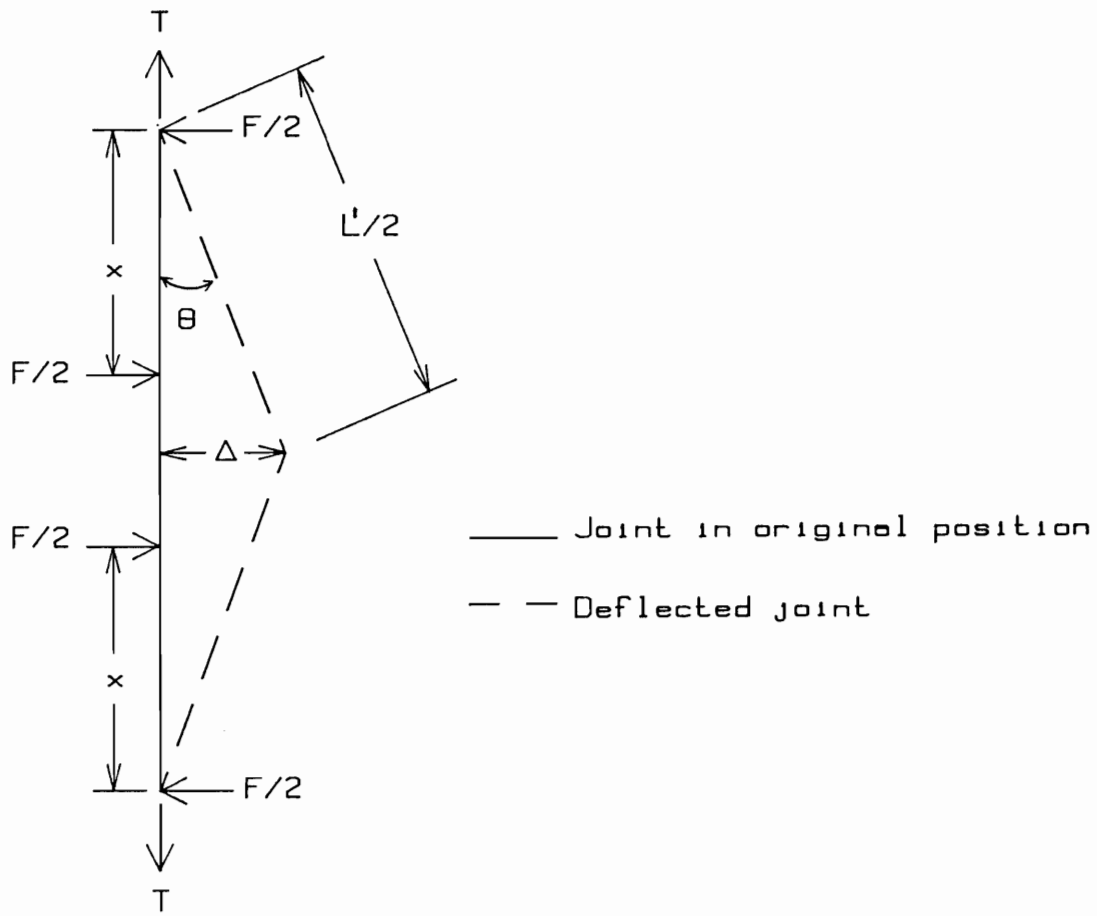

Where: x = the distance from the pinned support to the load bearing block

F = applied horizontal (bending) force

Figure 5.4 Free body diagram of the full scale joint under combined loading

It follows that:

$$M_{initial} = \frac{F}{2} * x \qquad (5.2)$$

and

$$M_T = T * \Delta \qquad (5.3)$$

and

$$M_{new} = \left(\frac{F}{2} * x\right) - \left(T * \Delta\right) \qquad (5.4)$$

Where: $M_{initial}$ = initial (target) bending moment

M_T = opposing moment due to tensile load

M_{new} = actual moment due to combined loading

In order to maintain the original target moment on the joint throughout the test, the bending force must therefore be continuously modified as follows:

$$\frac{F_{correcting}}{2} * x = T * \Delta \qquad (5.5)$$

$$F_{correcting} = \frac{2T\Delta}{x} = \frac{T(\sin\Theta * L')}{x}$$

The moment on the joint after a correcting force has been applied is therefore given by:

$$M_{target} = \left(\frac{(F_{initial} + F_{correcting})}{2} * x\right) - \left(T * \Delta\right) \qquad (5.6)$$

Expression 5.6 is used as the basis for controlling the lateral forces during the tests.

5.5 DATA ACQUISITION

As with the wafer technique, information necessary to describe the joints behavior during testing includes:

a. Tensile and bending forces

b. Rotation and elongation of the joint

The nature of data collection and control is similar to that used for the water test. Details of the computer program will therefore be omitted.

5.5.1 TENSILE AND BENDING FORCE MEASUREMENT

The load cell within the testing machine itself was used to record tensile forces. The output was directed to the computer for analog to digital conversion. Tensile loads were also visually monitored on the machine dial during the tests.

D.C. voltage outputs from the 300 pound load cell used to measure bending forces were similarly directed to the computer's data acquisition board.

5.5.2 JOINT ROTATION (θ) AND ELONGATION (ΔL) MEASUREMENT

In this study, ΔL is defined as the change in the total length of the joint due to bolt flexure and wood compression. Stretching of the wood fibers is not included in this definition and is not used in the calculations.

Joint rotation, θ, is defined here as the angle that is formed between a vertical line and the centerline of the

side members of the joint. It is calculated using a simplified bending diagram of the joint, shown as Figure 5.5.

Movements of the two horizontal arms (see Figure 5.3) relative to each other were measured and the results were used to infer deformation of the joint.

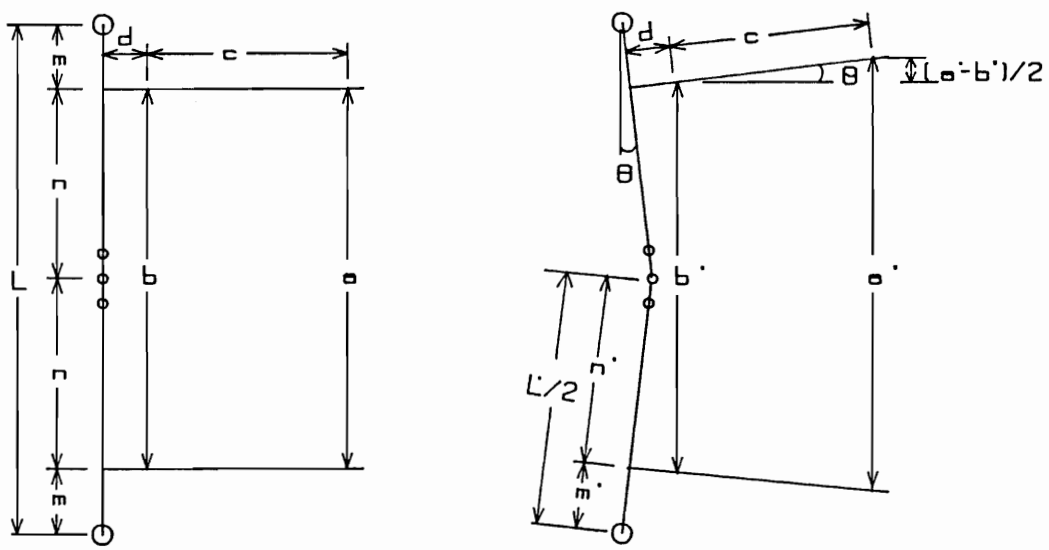

Joint in original position Deflected joint

where: a,b,c,d m,and n are constants.
a' and b' are measured by LVDTs.

Figure 5.5 Schematic representation of a whole joint and the horizontal measuring arms while the system is under test. Letters indicate the variables used to calculate joint elongation and rotation.

Initially, the arms were parallel to one another. As bending and tensile forces were applied to the members, the joint rotated and extended. Resultant movement of the joint could be inferred by measuring the vertical separation of the arms at two points along their length. Two 1/2" LVDTs were used for this purpose.

The rotation of the joint can be calculated as follows:

$$\sin\theta = \frac{\Delta a - \Delta b}{2c} \tag{5.7}$$

$$\theta = \sin^{-1}\frac{\Delta a - \Delta b}{2c}$$

where c = constant for the system (16" in this case).

Similarly, an expression for joint length, L', and joint elongation, ΔL, can be derived.

Given that:

$$L = 2m + 2n = 40"$$

where: m and n are constants

It follows that:

$$L' = 2m' + 2n' \tag{5.8}$$

and

$$\Delta L = L' - L \tag{5.9}$$

If one assumes elastic elongation of the members to be negligible, then:

$$m' = m = \text{constant}$$

and it is only necessary to calculate n'. It follows that:

$$n' = \frac{\frac{b'}{2} - d * \sin\theta}{\cos\theta} \qquad (5.10)$$

where $\sin\theta = \frac{\Delta a - \Delta b}{2c}$

Using the Pythagorean theorem, it follows:

$$\cos\theta = \frac{c}{\sqrt{c^2 - \left(\frac{(\Delta a - \Delta b)}{2}\right)^2}} \approx 1$$

for values of Δa and Δb considered.

Substituting $\frac{\Delta a - \Delta b}{2c}$ for $\sin\theta$, and 1 for $\cos\theta$ into equation 5.10 leaves:

$$n' = \frac{b'}{2} - \frac{d(\Delta a - \Delta b)}{2c} \qquad (5.11)$$

Substituting into equation 5.9 gives:

$$\Delta L = \left[2m' + 2\left(\frac{b'}{2} - \frac{d(\Delta a - \Delta b)}{2c}\right)\right] - (2m + 2n)$$

Recalling that m'= m and 2n = b, the equation simplifies to:

$$\Delta L = \Delta b - \frac{d(\Delta a - \Delta b)}{c} \qquad (5.12)$$

Expression 5.12 is used as the basis for calculating joint elongation.

5.6 DATA REDUCTION

The raw data stored on the disks did not require any corrections and was used as it was originally recorded. There was no friction to contend with, nor any corrections associated with alignment of the apparatus. Unlike the wafer approach, tensile load was not corrected for joint flexure since it was small and its effects were negligible.

Time constraints prevented combining and averaging data as was done with the wafer technique. The data presented in chapter VI is therefor shown in a different format than that for the wafer results.

Four types of curves were plotted after testing:

1. Tensile force versus elongation
2. Tensile force versus time
3. Bending force versus time
4. Bending moment versus time

Unavoidable electrical noise generated by some of the apparatus led to cyclical fluctuations in some tensile force vs. elongation curves. As with the wafer approach, peaks were connected with a straight line.

Because the properties of a complete bolted joint are directly dependent on the properties of the individual components that make up the joint, it is necessary to address bolted joint properties in terms of the whole system. The yield point, elasticity and proportional limit

of the system can be identified using these curves.

The bending force versus time curves were plotted to check the test conditions and were not used in data analysis.

Bending force versus time curves were compared to their moment versus time counterparts to see if increases in bending moment values were accurately reflected by increases in applied bending force.

The interaction between bending versus time, and tension versus time curves is complex. Bending and tensile forces are related by a sine function. An increase in tension should lead to an increase in measured bending force. If bending forces increase at a rate greater than this function, it indicates that permanent damage is being done to the joint; the joint is becoming weaker in bending and flexure will increase.

Applied bending moment versus time was plotted to check the experimental procedure. A consistent moment was to be maintained on the joint throughout the test. This curve enabled the accuracy of experimental control to be evaluated.

The results of these tests and their implications will be considered in conjunction with those from the wafer method in chapter VI to follow.

Chapter VI

RESULTS AND DISCUSSION

6.1 INTRODUCTION

This chapter summarizes the data from each of the two testing approaches. Statistical analysis is presented first, followed by a discussion of the load-displacement curves and a presentation of some comparisons between the two methods. Failure mechanisms are briefly discussed at the end of the chapter.

6.2 RESULTS FROM THE WAFER APPROACH

Results from this approach have been presented graphically and statistically. Figure 6.1 shows how the data has been organized for analysis.

6.2.1 STATISTICAL ANALYSIS

Two-way analysis of variance (ANOVA) was used to analyze the effects of wafer configurations and bending moments on both tensile load to failure and slope of the load-displacement curves. Analysis was performed using the "Number Cruncher" software package. A significance level of 0.05 is used throughout this section.

Table 6.1 summarizes the results of the analysis of the slope data. There was no significant interaction between the two factors (wafer configuration and bending

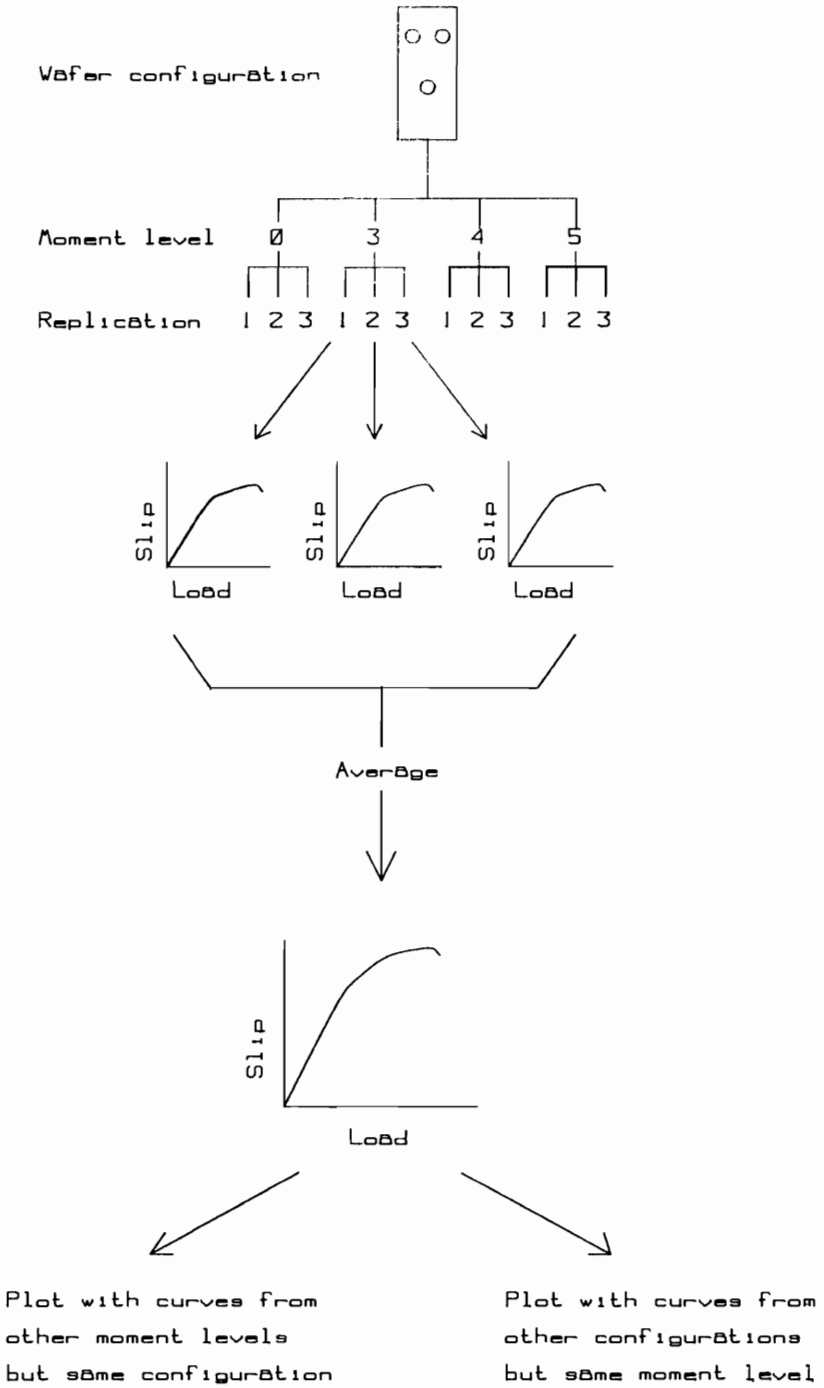

Figure 6.1 Schematic representation of how the raw data from the wafer approach was organized for analysis.

moment). The average slopes were compared using the Newman-Keuls method (22). Slopes which were found to be statistically similar are labeled with the same lower case letters in Table 6.1.

Table 6.1 A comparison of the mean slopes of the load-slip curves for each configuration/moment level tested. Lower case letters indicate which slopes were significantly different at the .05 level.

FACTOR		Avg. Slope (N/mm)		No. of Samples
Wafer Config.	Moment Level			
L-R	0	1111	a	4
L-R	3	1069	a	4
V-R	0	974	a	3
L-R	4	974	a	4
V-R	4	966	a	3
V-R	3	890	a	3
L-T	4	622	b	2
L-T	0	574	b	2
L-T	3	553	b	2

Table 6.2 summarizes the results of the analysis for the tensile load to failure data. More complete results of this analysis appear in appendix B. There was significant interaction between the two factors. Average tensile load to failure values were also compared according to Newman-Keuls method. Again, values which were found to be statistically similar are labeled with the same lower-case letter.

Table 6.2 A comparison of the mean tensile load to failure values for each configuration/moment level. Lower case letters indicate which loads were significantly different at the .05 level.

FACTOR		Avg. Tensile Load to Failure	No. of Samples
Wafer Config.	Moment Level		
V-R	0	971 a	3
L-R	0	936 a	4
V-R	3	904 a b	3
V-R	4	845 a b	3
L-T	0	735 a b	2
L-R	3	708 b	4
L-T	3	515 c	2
L-R	4	484 c d	4
V-R	5	412 c d	3
L-T	4	322 d	2
L-R	5	42 e	4
L-T	5	0 e	2

Section 6.2.2 considers these results in relation to load-displacement curves and maximum tensile loads.

6.2.2 FAMILY CURVES

Three types of curves have been plotted: 1) family of average load vs. displacement curves for each configuration, 2) family of average load vs. displacement curves for each moment level, and 3) tensile load to failure vs. bending moment for each configuration. Each curve will be discussed individually.

For each configuration, the effects of bending forces on the load-displacement characteristics of a wafer were seen by plotting a family of averaged tensile load vs. displacement curves. These appear as Figures 6.2 to 6.4.

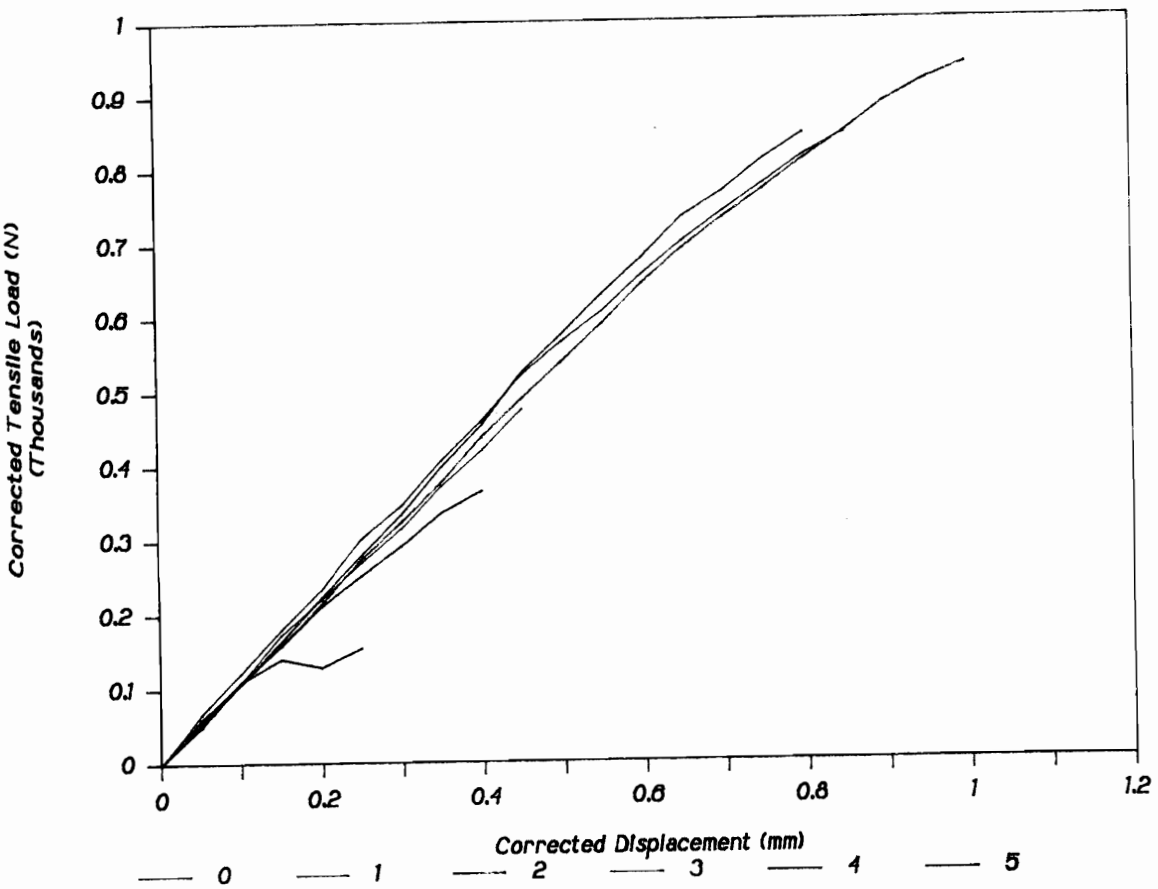

Where: 0 = moment level 0, no moment applied
1 = moment level 1, moment = 0*
2 = moment level 2, moment = 0*
3 = moment level 3, moment = 3.9 N m
4 = moment level 4, moment = 9.3 N m
5 = moment level 5, moment = 14.6 N m

* After correcting for friction

Figure 6.2 Family of average load-displacement curves for the "L-R" configuration. Each curve represents the average of 4 replications, with the exception of curve 5, which represents one test.

In Figure 6.2, each line represents the average of four test replications, with the exception of moment level 5. While four wafers were tested at this level, three broke in bending before the target moment was reached. The curve representing level 5 represents the one wafer which did not break before the target moment was reached.

The results shown in Table 6.1 indicate that the slopes of these averaged curves are not significantly different from one another at the .05 level. This implies that applied bending moments did not affect joint stiffness for this configuration.

On the other hand, average tensile load to failure was significantly reduced as bending moments were increased (see Table 6.2). This suggests that applied bending moments had an effect on the failure characteristics with this configuration.

The results from the "L-T" wafer configuration are shown in Figure 6.3. It should be noted that because of wafer availability, the number of replications was limited to two. There is no curve for bending moment level 5 because both wafers broke in bending before reaching the target moment.

Again, the slopes of these curves are statistically similar; applied bending moments did not affect joint stiffness. Average tensile load to failure was, again, significantly reduced as bending moments were increased (see Tables 6.1 and 6.2).

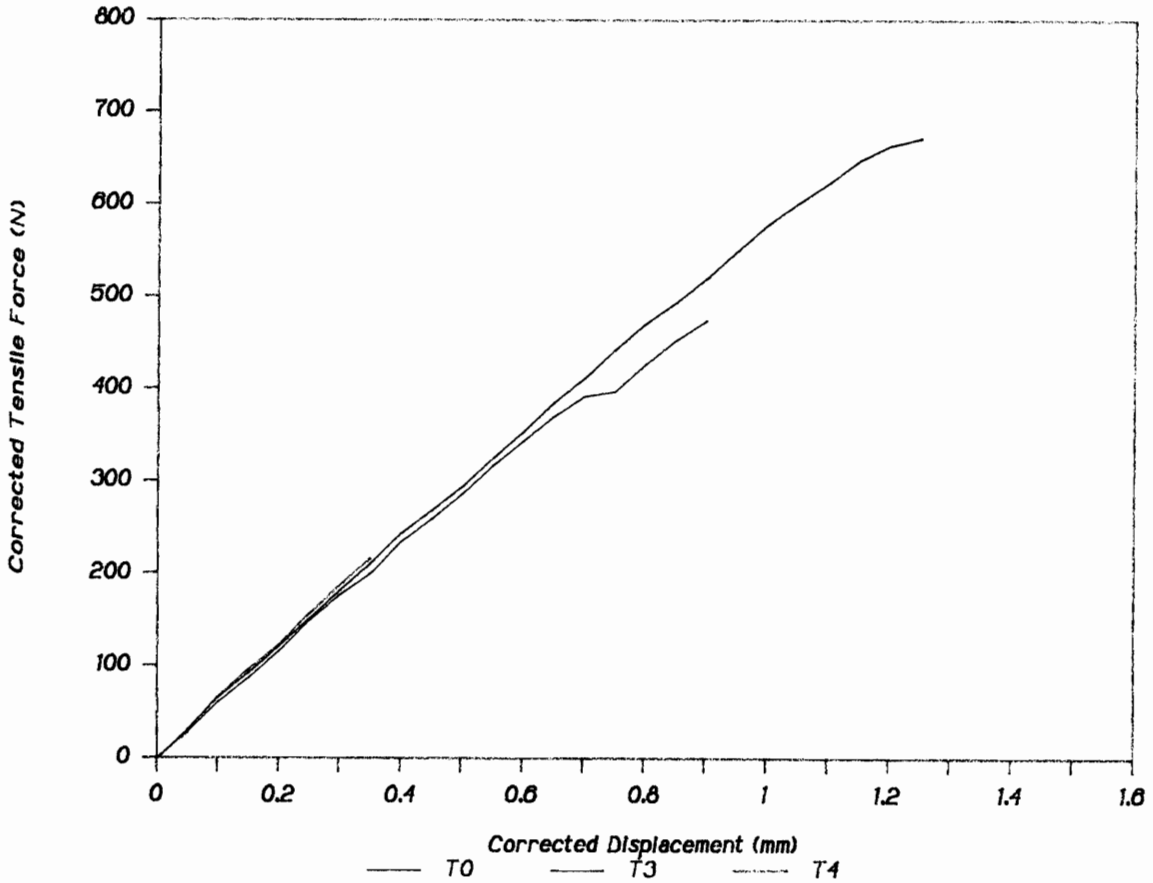

Where: T0 = moment level 0, no moment applied
T3 = moment level 3, moment = 4.5 N m
T4 = moment level 4, moment = 9.8 N m
T5 = moment level 5, moment = 15.2 N m

Figure 6.3 Family of average load-displacement curves for the "L-T" configuration. Each curve represents the average of 2 replications. Tests performed at moment level 5 broke before the target moment was reached.

Figure 6.4 shows the family of averaged load-displacement curves for the "V-R" configuration. Each line represents the average of three replications. The curve representing moment level 5 is noteworthy. Under this extreme bending moment, the horizontal displacement of the wafer and the horizontal forces required to maintain a constant moment exceeded the limits of the apparatus. The point where this occurred can clearly be seen on the load-displacement curves. The curves reach an apparent plateau and then begin to rise again when the limits of the system were exceeded. Had the moment level been maintained, failure would likely have occurred much sooner in the test.

Again, there is no significant difference between the slopes of the four curves. Similarly, bending moments did not have a significant effect on the tensile load to failure, except at the highest moment level. Compared to the wafers tested with the "L-R" or "L-T" configurations, the "V-R" configuration resulted in wafers which maintained their tensile strength, even at high moment levels. This implies that the "V-R" configuration may be less susceptible to the strength reducing effects of bending moments that the conventional linear configuration.

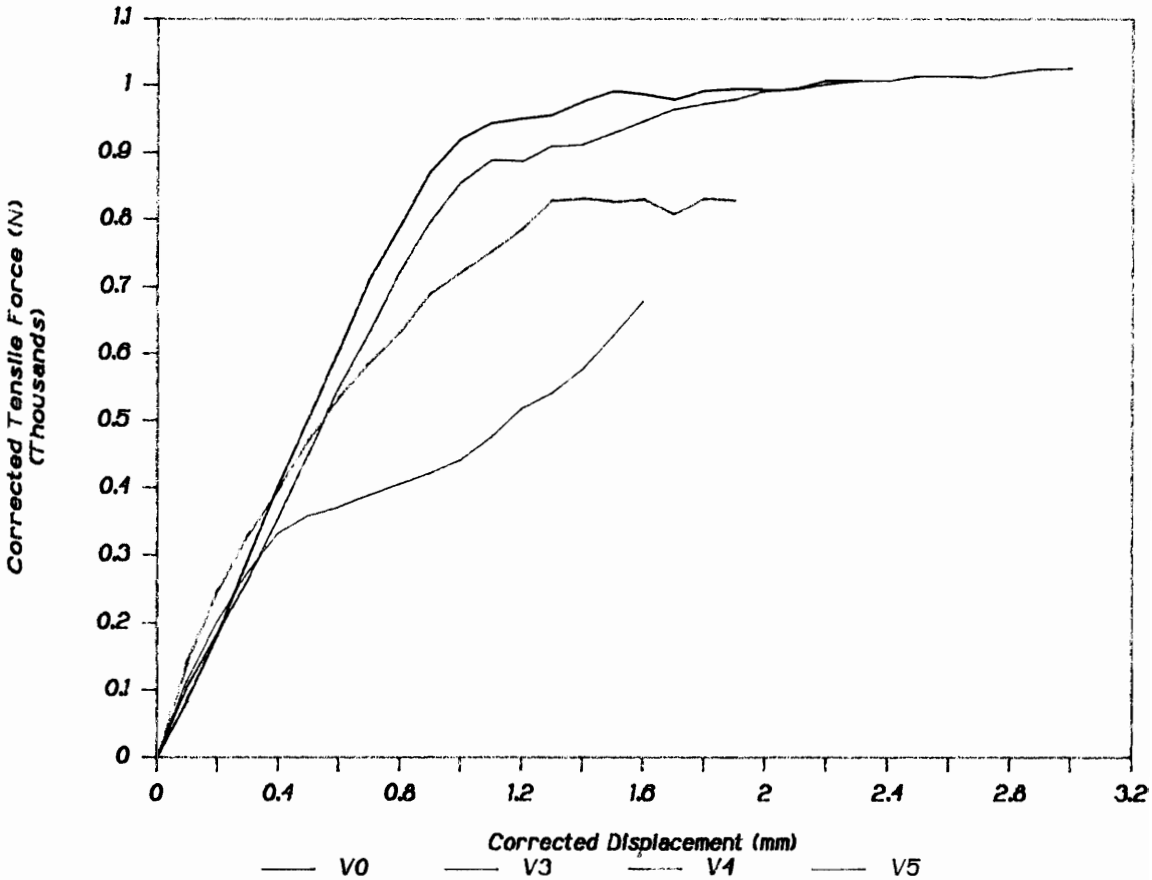

Where: V0 = moment level 0, no moment applied
V3 = moment level 3, moment = 4.5 N m
V4 = moment level 4, moment = 9.9 N m
V5 = moment level 5, moment = 15.2 N m

Figure 6.4 Family of average load-displacement curves for the "V-R" configuration. Each curve represents the average of 3 replications. The arrow indicates where the limits of the apparatus were exceeded.

Figures 6.5 to 6.8 have been plotted to make direct comparisons of the three configurations easier. One graph has been plotted for each bending moment level. The load-displacement curves from all three configurations are shown together on each graph.

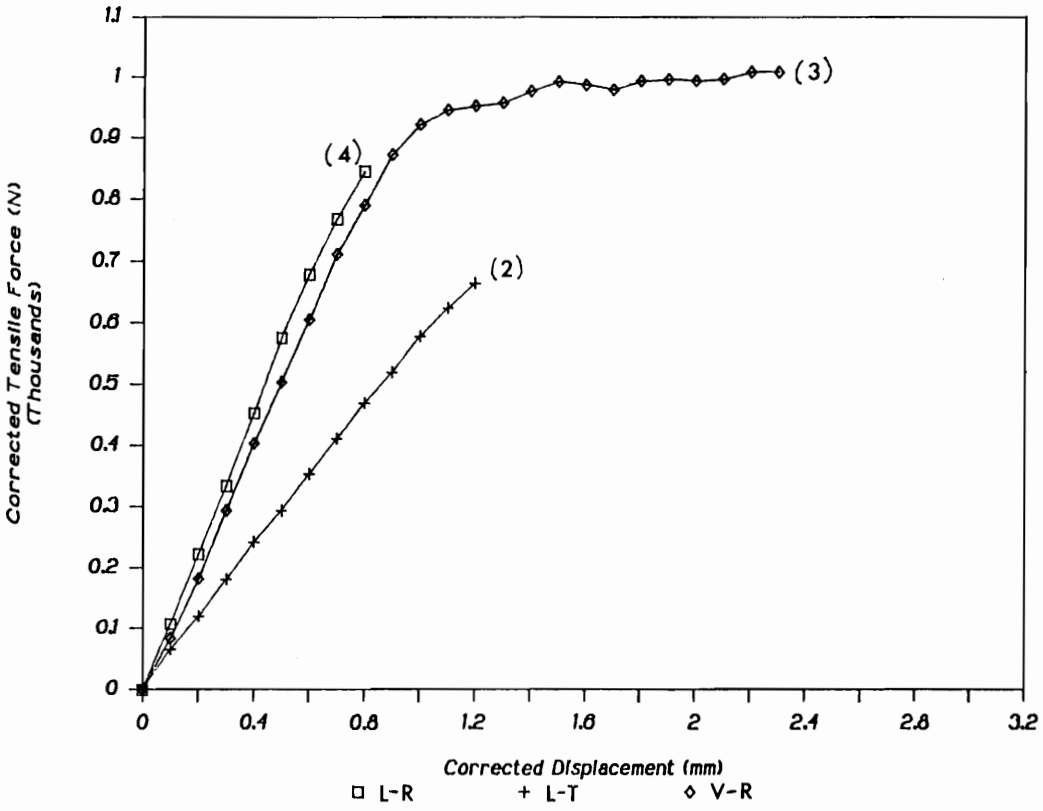

Figure 6.5 Averaged load-displacement curves for the three configurations when tested in tension only. The number of replications is indicated in parenthesis.

The slopes of the "L-R" curves and "V-R" curves are statistically equal in all cases. The slopes from these curves are, however, significantly steeper than the slopes of the "L-T" curves in all cases. This indicates that tangential wafers were more elastic than either of the radially oriented wafers.

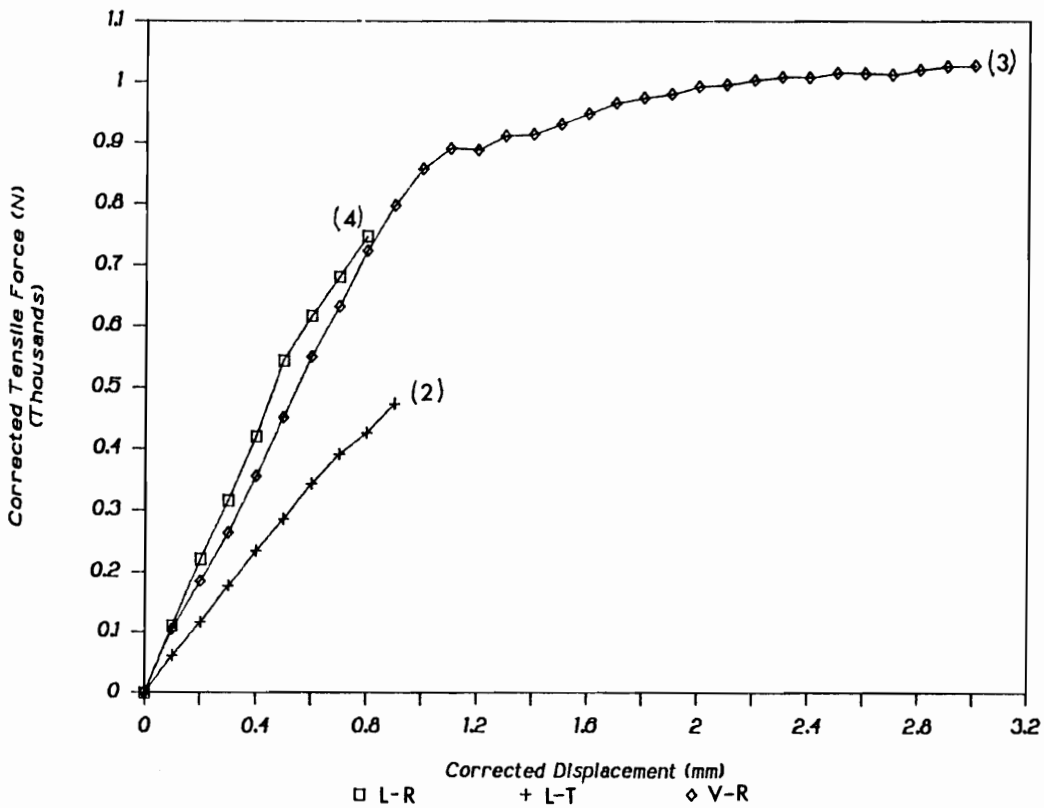

Figure 6.6 Averaged load-displacement curves for the three configurations when tested at moment level 3 (bending moment = 3.9 to 4.5 N·m). The number of replications is indicated in parenthesis.

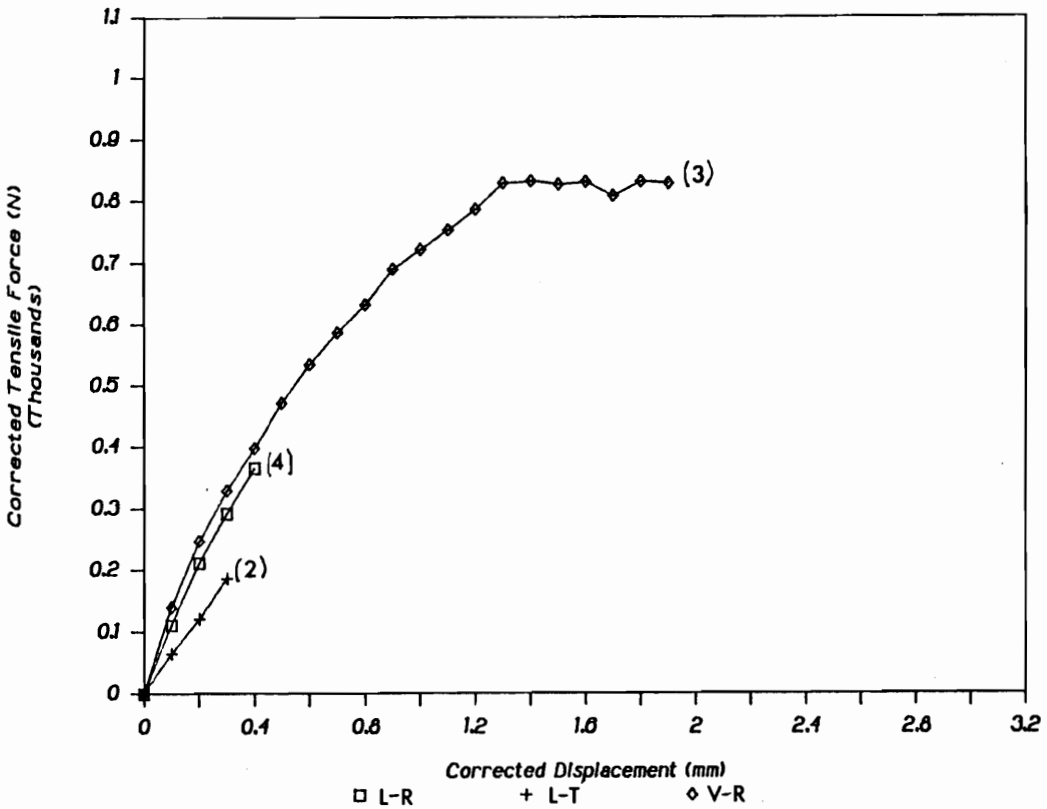

Figure 6.7 Averaged load displacement curves for the three configurations when tested at moment level 4 (bending moment = 9.3 to 9.9 N·m). The number of replications is indicated in parenthesis.

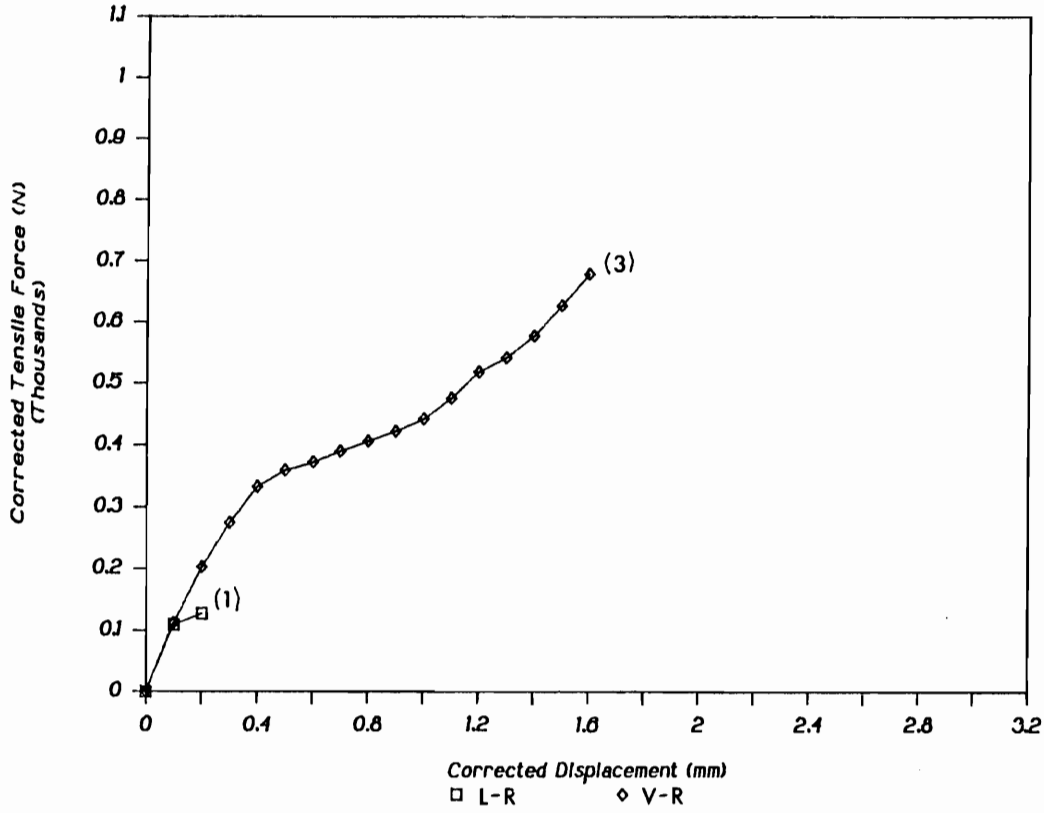

Figure 6.8 Averaged load-displacement curves for the three configurations when tested at moment level 5 (bending moment = 14.6 to 15.2 N·m). The number of replications is indicated in parenthesis.

For each configuration, average tensile load to failure was plotted against bending moment in Figure 6.9. When tested in tension only, there was no significant difference between the average tensile load to failure values for any of the configurations. At moment level 3, however, differences between the configurations become significant. In general, the wafers with the "V-R" configuration were the strongest while those with the "L-T" configuration were the weakest. Results are summarized in Table 6.2.

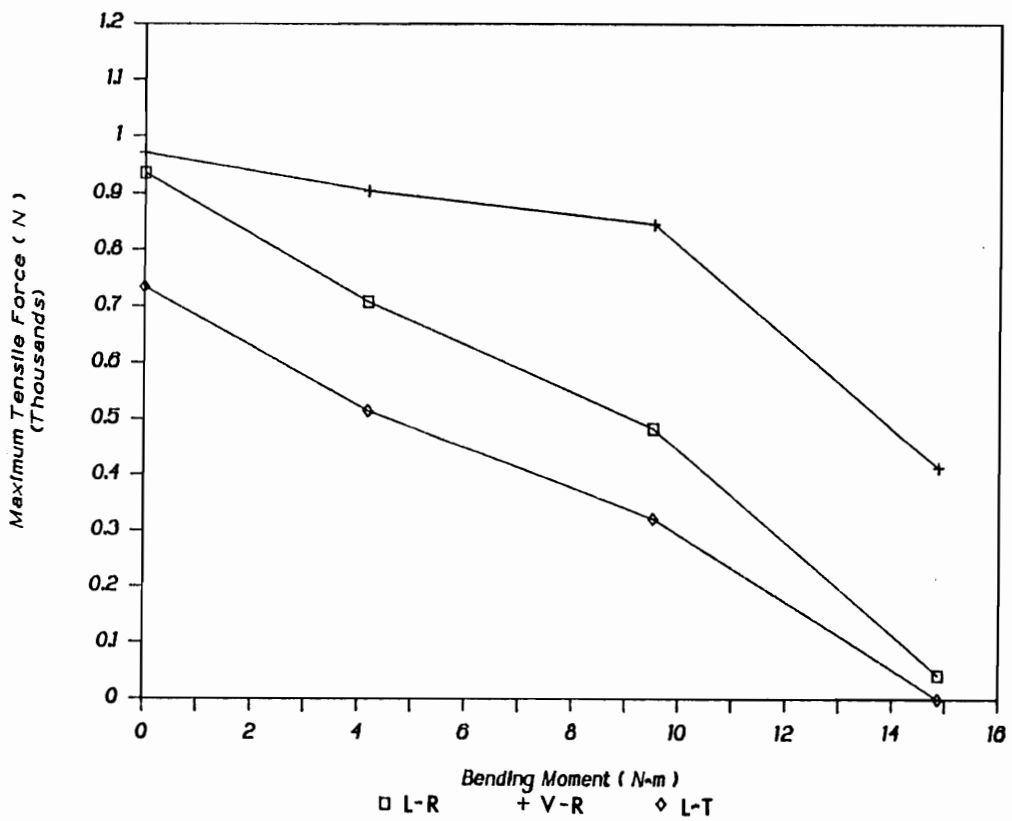

Figure 6.9 Average maximum tensile load to failure vs. bending moment for the three configurations.

Linear regression was used to fit lines through these points (regression lines are not shown). The resulting linear models appear in Table 6.3 along with the corresponding R^2 values. The high R^2 values for the "L-R" and "L-T" configurations indicate that there is a strong linear relationship between applied bending moments and tensile load to failure for these configurations. This may be due to the types of stresses produced with this configuration (see section 6.5).

Table 6.3 Linear regression models of the average tensile load to failure vs. bending moment for each of the three configurations.

Configuration	a	b	R^2
L-R	960	-58.4	0.88
V-R	1035	-35.3	0.78
L-T	736	-48.0	0.97

For the general linear model: $Y = a + bX$

Where: Y = Tensile load to failure (N)
a = Tensile load to failure when tested in tension only (N)
b = Slope (1/m)
X = Bending moment (N·m)

Table 6.3 indicates that configuration "L-R" has the steepest slope when tensile load to failure is plotted against bending moment. This implies that the "L-R" configuration may be more susceptible to the strength

reducing defects of bending moments than the other configurations. Possible reasons for this are considered in section 6.5.

6.3 RESULTS FROM THE FULL SCALE TESTING

Data from the full scale tests were analyzed using only tensile load to failure as a criteria. Results are summarized in Tables 6.4 and 6.5. Mechanical or data acquisition problems were encountered during some tests. These test results were not considered in the analysis. This caused uneven sample size and low replications at some moment levels and made a two way ANOVA unbalanced and impractical.

Figures 6.10 and 6.11 show the tensile load to failure vs. bending moment plots for joints made from both grades of lumber. Results from linear regressions through these points appear in Table 6.6. Both types of joints show the tendency for tensile load to failure to decrease as bending moment increases.

Table 6.4 Results of full scale testing of joints made with high grade material

Moment (N·m)	Max. Tensile Load (N)	Avg. Tensile Load (N)
0	64,350	
0	64,620	61,450
0	55,380	
595	59,160	
595	57,380	58,270
857	53,380	
857	50,040	
857	61,830	54,530
857	54,930	
857	52,450	
1143	45,370	-----
1236	6,290	-----

Table 6.5 Results of full scale testing of joints made with low grade material

Moment (N·m)	Max. Tensile Load (N)	Avg. Tensile Load (N)
0	61,160	
0	57,580	
0	42,480	56,760
0	65,830	
595	53,380	
595	36,030	
595	24,020	41,760
595	53,600	
857	28,690	
857	18,680	21,240
857	16,340	

Joints made from lower grade material indicate a definite inverse relationship between tensile strength and bending moment. This relationship may not be linear, however, as the R^2 value is somewhat low. The low R^2 value may also reflect the variability observed in the joints and not how well the model fits the data.

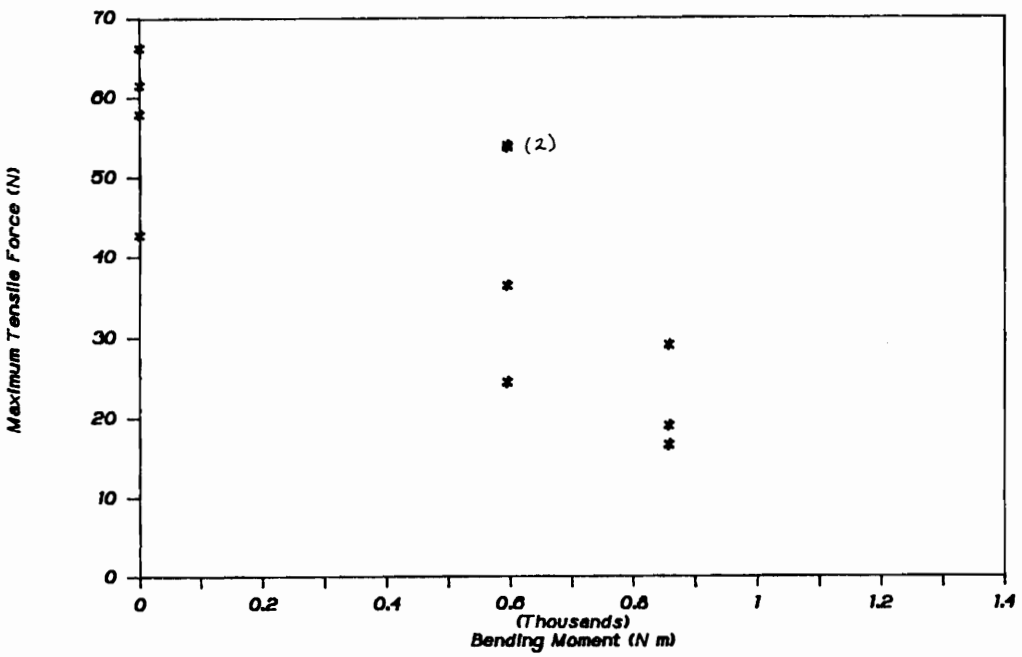

Figure 6.10 Plot of tensile load to failure versus bending moment for full scale joints made with low grade lumber.

The joints made from higher grade material produced different results. The slope of the regression curve was only slightly negative and the R^2 value was low. This implies that a linear relationship between bending moment and tensile load to failure is not well defined. The slightly negative slope suggests that joints made from high grade material are much less susceptible to the strength reducing effects of bending moments. Although this conclusion has not been confirmed statistically, it can be safely assumed that there will be some limiting bending moment value that will result in reduced tensile strength. More tests need to be conducted using higher grade material to better define the curve, especially at high moment levels.

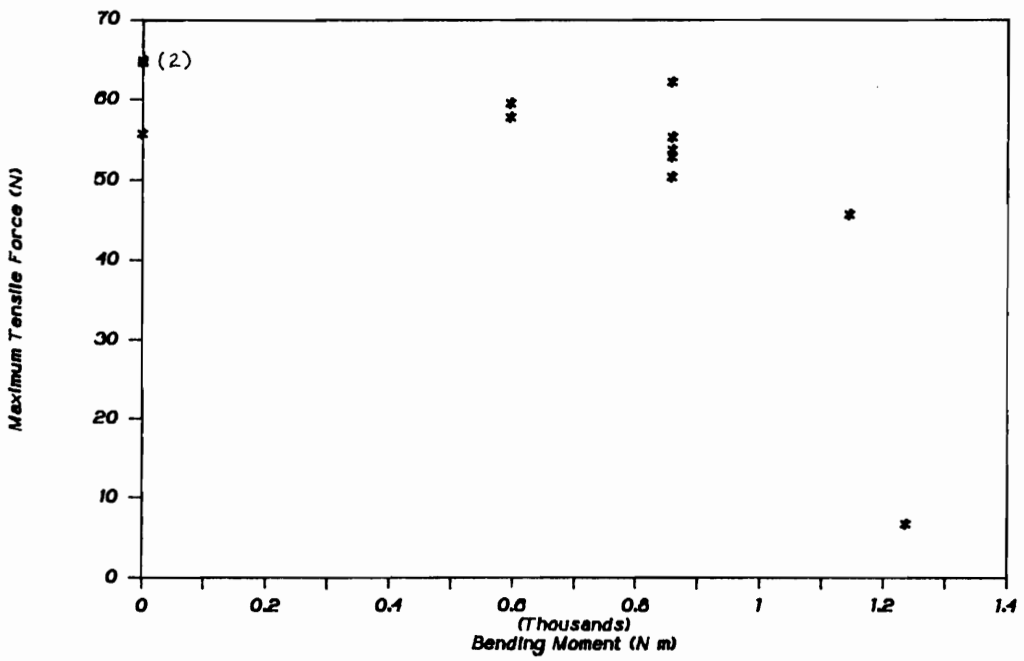

Figure 6.11 Plot of tensile load to failure versus bending moment for full scale joints manufactured with high grade lumber.

Table 6.6 Linear regression models of tensile load to failure vs. bending moment results for full scale joints.

Lumber Grade	a	b	R^2
High	61,714	-8.0	0.38
Low	58,464	-37.4	0.61

For the general linear model: $Y = a + bX$

Where: Y = Tensile load to failure (N)
a = Tensile load to failure when tested in tension only (N)
b = Slope (1/m)
X = Bending moment (N m)

The fact that the slopes of these two regression lines are so different suggests that the use of stress rated material may indeed enable joint strength and resistance to bending moments to be affected.

6.4 COMPARING THE TWO METHODS

The usefulness of the wafer approach depends on how well it can imitate a full size joint. One way to compare the two methods is to compare the effects of bending moment on tensile load to failure for both approaches. Figures 6.12 and 6.13 have been plotted for this purpose.

The wafer approach indicated there was a linear relationship between tensile load to failure and bending moment, whereas whole joint tests suggest that the relationship may be non-linear. Both techniques did show that as bending moment increases, tensile load to failure

decreases. From these preliminary studies, the wafer technique appears to imitate the behavior of joints made from low grade material better than it does those made from high.

Comparing the slopes of the regression lines from the two methods will provide some information as to how well the wafer approach models full size joints. (Only the

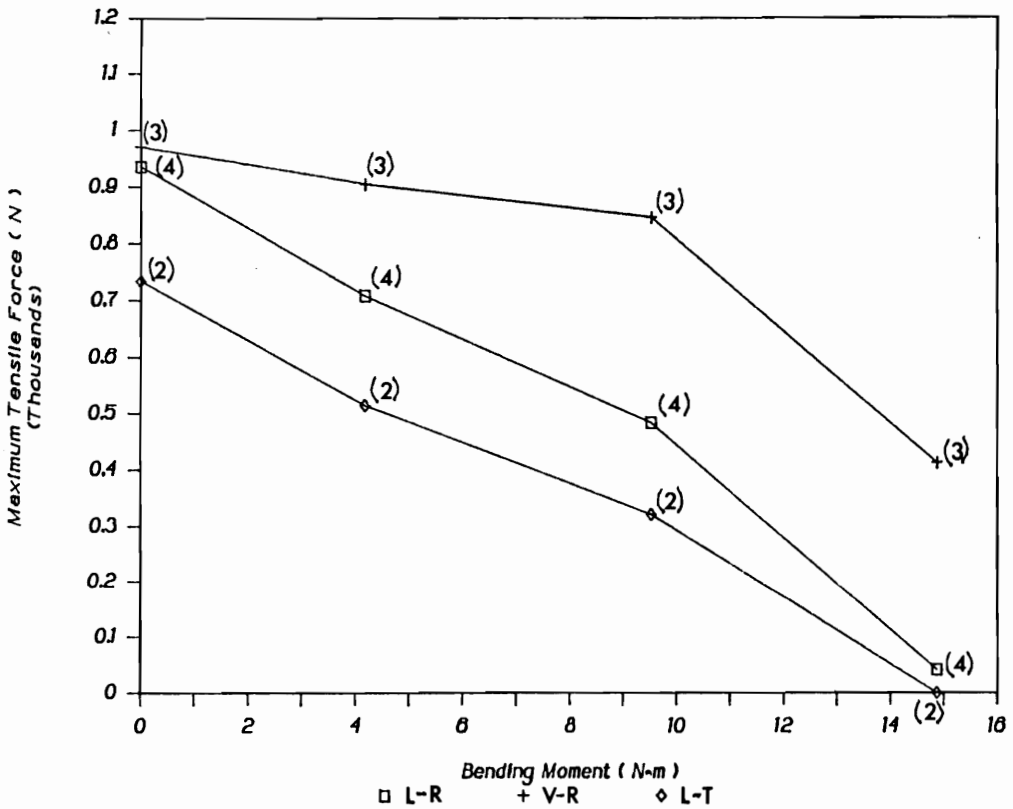

Figure 6.12 Average tensile load to failure vs. bending moment for each of the three wafer configurations. The number of replications is indicated in parentheses.

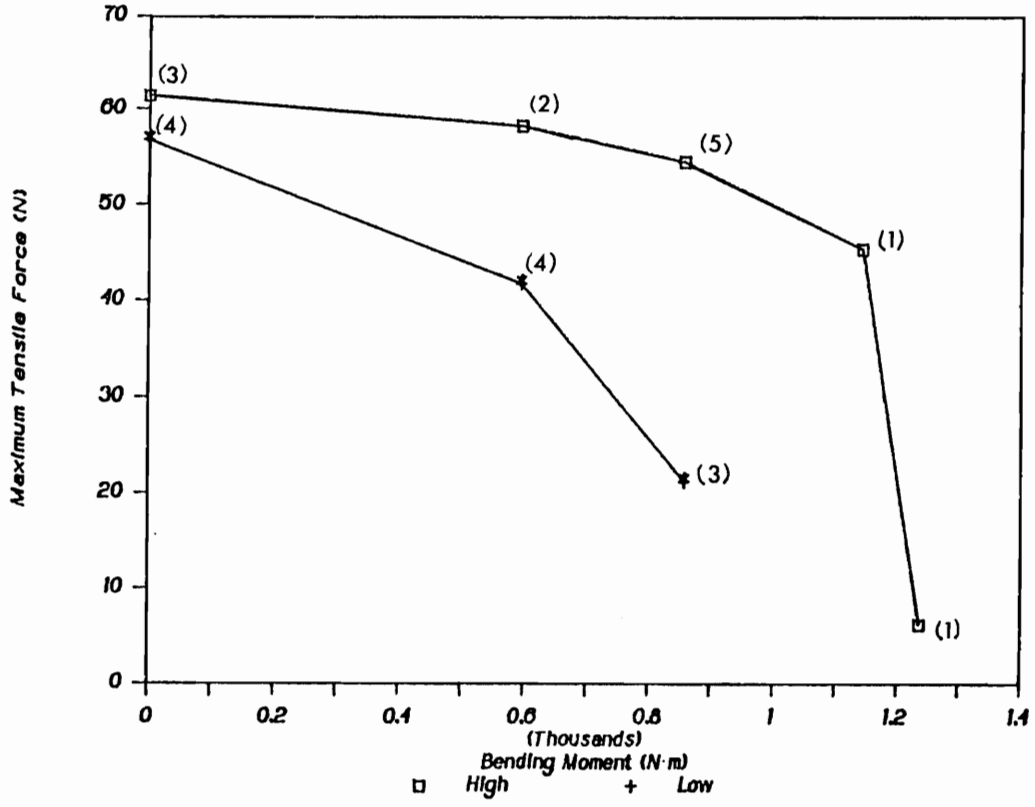

Figure 6.13 Average tensile load to failure vs. bending moment for both high and low quality joints. The number of replications is indicated in parenthesis.

"L-T" and "L-R" configurations can be directly compared to the full size joint results because the "V-R" configuration was not tested in full scale joints.)

In general, the slopes of the regression lines from the "L-T" and "L-R" configurations are steeper than those obtained from full scale testing. If this criteria is used to evaluate the effectiveness of the wafer technique, the "L-T" configuration appears to be a more accurate model of the full size joint.

Neither of the two configurations ("L-R" or "L-T") showed the high resistance to bending moments that was exhibited by the high strength joints. This implies that the wafer approach is more sensitive to the effects of bending moments on joint strength. The general trends do, however, agree with the full size test and are promising.

Results from the wafer technique for the "V-R" configuration imply that full size joints using a triangular bolt configuration would maintain high tensile strength even at high moment levels.

Another possible way to roughly compare the two methods is to correct for size differences that exist between the wafer and full size joint. The average thickness of the wafers was .84 mm, 91 times thinner than the main member in the full scale joints used. If the wafers were to model a full size joint perfectly, then multiplying the tensile load to failure values obtained from the wafers by 91 should give the same results as the full size tests. Listed below in Table 6.7 are the regression equations from the wafer approach corrected for thickness by multiplying the Y intercept by 91. Equations from the full scale test also appear for comparison.

Using this model, the wafer technique overestimates the maximum tensile strength of full scale joints when there is no moment on the joint.

Table 6.7 A comparison of the linear regression models derived from the wafer technique and the full scale tests. The intercepts of the wafer models have been multiplied by a factor of 91 to correct for size.

Wafer Configuration	a	b	R^2
L-R	87353	-58.4	.88
V-R	94229	-35.3	.78
L-T	66939	-48.0	.97
Full Scale Wood Quality			
High	61714	- 8.0	.38
Low	58464	-37.4	.61

For the general linear model: $Y = a + bX$

Where: Y = Tensile load to failure (N)
a = Tensile load to failure when tested in tension only (N)
b = Slope ($1/m$)
X = Bending moment (N·m)

Clearly, this approach is very approximate and takes no account for the complex distribution of strains that occur along the length of bolts in a joint which is loaded.

Generally, tensile load to failure values varied more with the full size joints than with the wafer joints. Variation in full scale joints can come from several sources. Wood material properties vary along the bolt axis. Because there is more material in full size joints, there is also the potential for more defects or "weak links" in the system. The wafer approach removes much of

this variation by reducing it to two dimensions. Thus, results from full scale tests can realistically be expected to have more variation than results from the wafer technique.

The complex interaction of the components that make up a full scale bolted joint add to the variability. Bolt flexure, hole tolerance, and hole alignment are difficult to accurately control in a full scale joint. Some of these factors, such as bolt flexure, are not accounted for with the wafer approach. While this may alter the model, it is one of the main advantages of the wafer method. By being able to remove some of the variables within a joint, this method can provide more fundamental information on the behavior of material within a joint as it is loaded.

6.5 FAILURE MECHANISMS

The roles of grain orientation, bolt configuration and load combinations in determining joint failure modes are each briefly discussed in turn.

Effect of grain orientation:

In Douglas-fir, the growth rings are very distinct and the transition from earlywood to latewood is abrupt. Because of the anatomical differences between earlywood and latewood, shear stress tended to concentrate at their interfaces. This stress concentration appeared to play the the greater role in radially cut wafers where tensile

forces perpendicular to the grain acted in the radial direction. Some effects of grain orientation on failure mechanisms can be seen by comparing Figures 6.14 (a) and 6.15 (a).

Effect of load combinations:

When tensile loads were applied to the joints, four predominant modes of stress were developed. Compression stresses perpendicular to the grain were transferred from the sides of the bolts and these produced tension perpendicular to grain stresses which tended to cause the wood to split. Shear stresses were developed in the regions above and adjacent to the bolts. Compression parallel to grain failures occurred as the wood crushed above the bolts.

Moment = 0 Moment = 3.9 N·m

Figure 6.14 Photographs of typical failures at different bending moment levels for wafers using the "L-R" configuration

Moment = 9.3 N·m

Moment = 14.6 N·m

Figure 6.14 continued

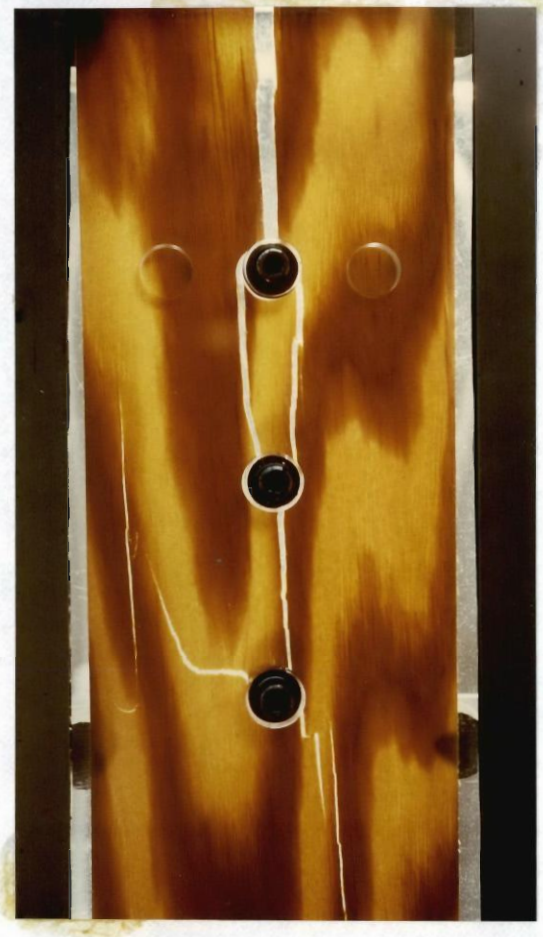

Moment = 0

Moment = 15.2 N·m

Figure 6.15 Photographs of typical failures in tangentially cut wafers ("L-T" configuration)

Joints with linear bolt configurations were very stiff in tension. Consequently, compressive deformation parallel to the grain did not appear to significantly affect joint failure. (This is in contrast to Ostman's work on single bolt joints (18).) Multiple bolted joints loaded in tension tended to fail in shear mode, (see Figure 6.14 (a) and Figure 6.16).

Figure 6.16 Shear failure in full scale joint loaded in tension

Bending forces primarily caused tension and compressive stresses perpendicular to the grain. Because wood is weaker in tension perpendicular to the grain than it is parallel to the grain, the stresses added due to the bending moment often changed the failure mode. One would expect joints tested under bending loads alone to be more likely to split, rather than shear, as a result of tension perpendicular to grain stresses. This was indeed observed with both the wafer technique and in the full scale testing. Figure 6.14 (d) shows a typical failure observed for a wafer under pure bending.

Under combined loading, the failure mode became a combination of shear and splitting. As the bending force increased, tension perpendicular to the grain increased, and the mode of failure shifted from a shear mode to a splitting mode. This is clearly seen in Figures 6.14 (a) to (d) which show typical failure modes with the "L-R" configuration at each moment level. The failure modes for the "V-R" configuration were similarly affected by bending moments, although the pin configuration tended to offset these effects somewhat (see Figure 6.17). The trends were not as evident with the tangentially cut wafers (see Figure 6.15).

A complete set of photos was not available for the full scale tests, however, the observed failure characteristics were similar under corresponding conditions.

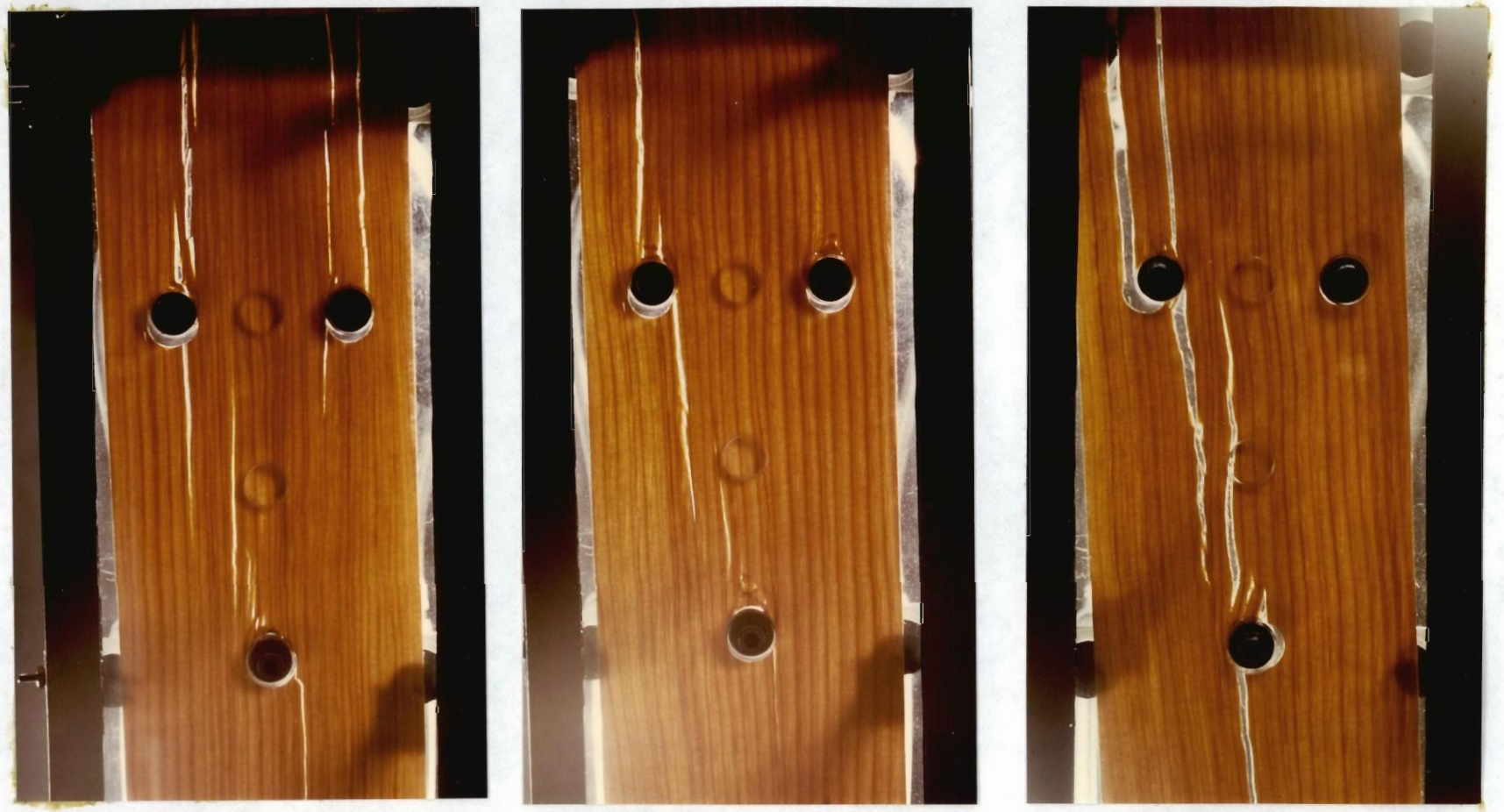

Moment = 0 Moment = 9.9 N·m Moment = 15.2 N·m

Figure 6.17 Photographs of typical failures at different bending moment levels for wafers with the "V-R" configuration

The effect of bolt configuration:

Under tensile loading, the conventional linear arrangement causes shear stress to be concentrated in a very narrow zone above the line of bolts. This configuration also results in high tension perpendicular to grain stresses when bending loads are applied. Results from the wafer tests and full scale testing confirm this. Joints using this configuration typically failed in shear when loaded in tension. When high bending loads were applied, the failure mode shifted to splitting.

For this reason, the standard bolt configuration was altered in an attempt to improve the joint performance- particularly with regard to susceptibility to bending moments. Several alternative geometries were considered before the triangular "V-R" design was chosen. This configuration reduced the concentration of shear stresses that are produced above the pins. This resulted in joints that were less susceptible to early shear failures. Typically, these joints failed initially in compression parallel to grain. Eventually, shear or splitting forces caused catastrophic failure.

Possibly of greater importance is the dispersion of stresses perpendicular to grain that are caused by the bending force. Results of preliminary tests using the "V-R" configuration with the wafer technique suggest that this is indeed the case. These joints showed significantly less susceptibility to bending moments.

The mode in which the joints ultimately failed depended on the interrelated effects of growth ring orientation, load direction and bolt configuration.

Chapter VII

CONCLUSIONS AND RECOMMENDATIONS

7.1 INTRODUCTION

This work concerned the development of techniques to investigate the behavior of multiple bolted joints when subjected to combined loading. Two techniques were employed. The wafer technique was designed to model a full scale joint and provide basic information on multiple bolted joints. The full scale approach was used to provide empirical information and to verify results from the wafer technique.

7.2 CONCLUSIONS

The wafer technique:

1. The technique can be used to produce combined loading conditions that correspond to those that may occur within real joints.

2. Bending moments had significant effects on the tensile load to failure characteristics of some configurations. Using wafers with the linear pin arrangement, tensile load to failure was significantly decreased as bending moments were increased. The relationship appears to be linear (R^2 values were 0.97 and 0.88).

3. Bending moments did not significantly affect the stiffness of the wafer joints.

4. Grain orientation affected joint behavior. Model joints with tangentially cut wafers were less stiff than those with radially cut wafers. Joints with radially cut wafers and the linear pin configuration were stronger in tension than those with tangentially cut wafers.

5. Modifying bolt configuration significantly affects joint behavior. The triangular pin configuration produced joints that were less susceptible to bending moment effects than the linear configuration. The triangular configuration has the potential to produce stronger joints.

6. The wafer technique has potential for being used as a tool to study the effects of other bolt geometries on joint behavior.

Whole joint testing:

7. Lumber grade may affect the susceptibility of joints to bending moments. Full scale joints made with lower grade material showed a decrease in tensile load to failure when bending moments were increased, though the relationship is more complex than the linear effect detected with the wafer technique.

7.3 RECOMMENDATIONS

1. Additional full scale joints should be tested at higher bending moment levels to better define the tensile load to failure/bending moment relationship.

2. Full scale joints should be tested using the triangular bolt configuration. This information would prove useful in verifying the results from the wafer technique. Stronger joints which are less susceptible to bending moments may result.

3. A wide range of new bolt geometries need to be studied to enable significant improvements in overall performance to be realizes.

BIBLIOGRAPHY

1. American Society for Testing and Materials, "Standard Methods of Static Tests of Timbers in Structural Sizes". American Standards for Testing and Materials Designation D198-84, 1984.

2. Bohannan, B. Prestressed laminated wood beams. U.S. Forest Products Lab. Research Paper No. FPL 8. 1964.

3. Cramer, C.O. Load distribution in multiple-bolt tension joints. ASCE, Vol. 94, No. ST5, Proc. Paper 5939. pp. 1101-1117. May, 1968.

4. Dannenberg, L.J., and R.G. Sexsmith. Shear-plate load distribution in laminated timber joints. Report No. 361. Dept. of Structural Engineering, School of Civil and Environmental Engineering. Cornell University. July, 1976.

5. Doyle, D.V. Performance of joints with eight bolts in laminated Douglas-fir. U.S. Forest Products Lab. Research Paper No. FPL 10. 1964.

6. Goodman, J.R., and M.E. Criswell. Changes in design philosophy. FPRS Symposium Proceedings: Wall & floor systems - Design and performance of light-frame structures. Denver, CO. 1981.

7. Gromola, D.S., and A. Polensek. Analysis and design of wall systems under axial and bending loads. FPRS Symposium Proceedings: Wall & floor systems - Design and performance of light-frame structures. Denver, CO. 1981.

8. Hirai, T. Effect of loading direction on the bearing characteristics of wood under a bolt. Journal of the Japan Wood Research Society 30(12):959-964. 1984.

9. Hirai, T., and K. Horie. Lateral resistance of bolted wood-joints with steel side-members. Journal of the Japan Wood Research Society 30(12):965-972. 1984.

10. Hudson, W.M. The effect of pre-compression on the static and impact bending strength of wood. Wood (London) 26(1):18-20. 1961.

11. Isyumov, N. Load distribution in multiple shear plate joints in timber. Publication No. 1203. Dept. Of Forestry. Ottawa, Ontario, Canada. 1967.

12. Kunesh, R.H., and J.W. Johnson. Strength of multiple-bolt joints: Influence of spacing and other variables. Report T-24. Department of Forest Products, School of Forestry. Oregon State University. March, 1968.

13. Lantos, G. Load distribution in a row of fasteners subjected to lateral load. Wood Science 1(3):129-136. 1969.

14. McLain, T.E. Influence of metal side plates on the strenght of bolted wood joints. Subcommittee on Structural Design and Engineering Properties. Madison, WI. February, 1983.

15. National Design Specification for Wood Construction. National Forest Products Association. Washington, D.C.. 1982.

16. Newlin, J.A., and G.W. Trayer. Stresses in wood members subjected to combined column and beam action. U.S. Forest Products Lab. Research Report No. 1311. 1956.

17. Norris, C.B. Strength of orthotropic materials subjected to combined stresses. U.S. Forest Products Lab. Research Report No. 1816. 1962.

18. Ostman, L. Development of techniques to study the behavior of bolted wood joints. Masters Thesis. Department of Forest Products. Oregon State University. Corvallis, Oregon. 1985.

19. Peterson, J. Wood beams pre-stressed with bonded tension elements. ASCE. Vol. 91, No. ST-1. February, 1965.

20. Senft, J.F. Further studies in combined bending and tension strength of structural 2 by 4 lumber. Forest Products Journal 23(10):36-41. 1973.

21. Senft, J.F., and S.K. Suddarth. Strength of structural lumber under combined bending and tension loading. Forest Products Journal 20(7):17-21. 1970.

22. Snedecor, G.W., and W.G. Cochran. Statistical Methods, 7th Edition. The Iowa State Community Press. Ames, Iowa. 1980

23. Snodgrass, J.D., and W.W. Gleaves. Effect of end-distance on strength of single-bolt joints. Subcommittee on Structural Design and Engineering Properties. Madison, WI. February, 1983.

24. Thangjitham, S. A method of evaluating the probabalistic resistance of bolted wood joints. Masters Thesis. Department of Forest Products. Virginia Polytechnic Institute. Blacksburg, Virginia. 1980.

25. Trayer, G.W. The bearing strength of wood under bolts. U.S. Dept. of Agriculture, Technical Bulletin No. 332. 1932.

26. Wilkinson, T.L. Assessment of modification factors for a row of bolts or timber connectors. U.S. Forest Products Lab. Research Paper No. FPL 376. 1980.

27. _____. Design factors for a row of fasteners in wood. U.S. Forest Products Lab. Manuscript in preparation. 1983.

28. _____. Load distribution among bolts in a row. U.S. Forest Products Lab. Manuscript in preparation. 1983.

29. Wilkinson, T.L., and R.E. Rowlands. Analysis of Mechanical joints in wood. Experimental Mechanics (11):408-414. 1981.

30. Zahn, J.J. Strength of lumber under combined bending and compression. U.S. Forest Products Lab. Research Paper No. FPL 391. 1982.

APPENDICES

APPENDIX A

The computer program used for data acquisition with the wafer technique is shown below. For the investigation of full scale joints, the program was modified slightly.

```
10 '    M T S G O . B A S
20 '    **********************
21 '
22 '    This program collects data using the Data Translation 2805 board.
23 '    It is based on the program MANEP07.BAS.
24 '
25 '
80 '
90 'define constants
100 '
110 DEFINT A-Z
120 BASE.ADDRESS       =&H2EC
130 COMMAND.REGISTER   =BASE.ADDRESS+1
140 STATUS.REGISTER    =BASE.ADDRESS+1
150 DATA.REGISTER      =BASE.ADDRESS
170 COMMAND.WAIT       =&H4
180 WRITE.WAIT         =&H2
190 READ.WAIT          =&H5
200 '
210 CCLEAR             =&H1
220 CCLOCK             =&H3
230 CSAD               =&HD
240 CRAD               =&HE
250 CSTOP              =&HF
260 PERIOD#            =60000!
270 '
280 BASE.FACTOR#       =4096
285 BASE.CHANNELS      =8
289 DIM GAIN(5)
290 GAIN(0)            =1
291 GAIN(1)            =10
292 GAIN(2)            =100
293 GAIN(3)            =500
300 '
310 'stop and clear the dt2801 series board
320 '
330 OUT COMMAND.REGISTER, CSTOP
340 TEMP = INP(DATA.REGISTER)
350 WAIT STATUS.REGISTER, COMMAND.WAIT
360 OUT COMMAND.REGISTER, CCLEAR
1000 '
1010 'set clock rate
1020 '
1030 'wait until the dt2801 board ready flag is set, then write the
1040 'set clock period command byte to the command register
```

```
1050 '
1060 WAIT STATUS.REGISTER, COMMAND.WAIT
1070 OUT COMMAND.REGISTER, CCLOCK
1080 '
1090 'divide period# into high and low bytes and write both bytes to the data
1100 'in register, waiting for a clear data in full flag before each write.
1110 '
1130 PERIODH# =INT(PERIOD#/256)
1140 PERIODL# = PERIOD# - PERIODH#*256
1150 WAIT STATUS.REGISTER , WRITE.WAIT,WRITE.WAIT
1160 OUT DATA.REGISTER, PERIODL#
1170 WAIT STATUS.REGISTER, WRITE.WAIT, WRITE.WAIT
1180 OUT DATA.REGISTER, PERIODH#
1190 '
1191 PRINT "RUN NAME ( ... ...) EQUALS ?";
1192 INPUT NRUN$
1193 PRINT "SCANNING TIME (SECONDS) EQUALS ?";
1194 INPUT TTIME#
1195 PRINT "TARGET PRESSURE EQUALS ?";
1196 INPUT TARGET!
1197 PRINT "ZERO LOAD VOLTAGE EQUALS?";
1198 INPUT VOLTAGE!
1270 ADGAIN =0
1280 PRINT "A/D START channel ( 1 TO 7 )";
1282 INPUT ADSCHANNEL
1290 IF ADSCHANNEL<0 THEN GOTO 1280
1300 IF ADSCHANNEL > (BASE.CHANNELS-1) THEN GOTO 1280
1310 '
1320 PRINT "A/D END CHANNEL ( 1 TO 7 )";
1325 INPUT ADECHANNEL
1330 IF ADECHANNEL <0 THEN GOTO 1320
1340 IF ADECHANNEL >(BASE.CHANNELS-1) THEN GOTO 1320
1360 NCHAN = ADECHANNEL - ADSCHANNEL + 1
1370 IF NCHAN < 1 THEN NCHAN = NCHAN + BASE.CHANNELS
1380 NCONVERSIONS# = TTIME#/.15
1400 '
1410 'DIMENSION ARRAY TO HOLD HIGH AND LOW BYTE OF A/D DATA.
1420 '
1430 DIM ADL(4200), ADH(4200)
1440 '
1450 'DO A SET A/S PARAMETERS COMMAND TO SET UP THE A/D CONVERTER.
1460 '
1470 'WAIT UNTIL THE DT2801 BOARD READY FLAG IS SET THEN WRITE THE
1480 'SET A/D PARAMETERS COMMAND BYTE TO THE COMMAND REGISTER.
1490 '
1500 WAIT STATUS.REGISTER, COMMAND.WAIT
1510 OUT COMMAND.REGISTER, CSAD
1520 '
1530 'WAIT UNTIL THE DT2801 BOARD DATA IN FULL FLAG IS CLEAR, THEN
1540 'WRITE THE A/D GAIN BYTE TO THE DATA IN REGISTER.
1550 '
1560 WAIT STATUS.REGISTER, WRITE.WAIT, WRITE.WAIT
1570 OUT DATA.REGISTER, ADGAIN
1580 '
```

```
1590 'WAIT, UNTIL THE DT2801 BOARD DATA IN FULL FLAG IS CLEAR, THEN
1600 'WRITE START CHANNEL BYTE TO THE DATA REGISTER.
1610 '
1620 WAIT STATUS.REGISTER, WRITE.WAIT, WRITE.WAIT
1630 OUT DATA.REGISTER, ADSCHANNEL
1640 '
1650 'WAIT UNTIL THE DT2801 BOARD DATA IN FULL FLAG IS CLEAR, THEN
1660 'WRITE THE A/D END CHANNEL BYTE TO THE DATA REGISTER.
1670 '
1680 WAIT STATUS.REGISTER, WRITE.WAIT, WRITE.WAIT
1690 OUT DATA.REGISTER, ADECHANNEL
1700 '
1710 'DIVIDE NCONVERSIONS# INTO HIGH AND LOW BYTES AND WRITE BOTH BYTES
1720 'TO THE DATA IN REGISTER, WAITING FOR A CLEAR DATA IN FULL FLAG
1730 'BEFORE EACH WRITE.
1740 '
1750 NUMBERH= INT(NCONVERSIONS#/256)
1760 NUMBERL= NCONVERSIONS#-NUMBERH*256
1770 WAIT STATUS.REGISTER, WRITE.WAIT, WRITE.WAIT
1780 OUT DATA.REGISTER, NUMBERL
1790 WAIT STATUS.REGISTER, WRITE.WAIT, WRITE.WAIT
1800 OUT DATA.REGISTER, NUMBERH
1810 '
1820 'START  THE READ A/D COMMAND.
1830 '
1840 'WAIT UNTIL THE DT2801 BOARD READY FLAG IS SET, THEN  WRITE THE
1850 'A/D COMMAND BYTE TO THE COMMAND REGISTER.
1860 '
1870 WAIT STATUS.REGISTER, COMMAND.WAIT
1880 OUT COMMAND.REGISTER, CRAD
1890 '
1900 'READ THE A/D, HIGH AND LOW BYTES, INTO ARRAYS, WAITING FOR A SET
1910 'DATA OUT READY (OR READY) FLAG BEFORE EACH READ.
1920 '
1921 PRINT "!!!!!DATA COLLECTION STARTED !!!!!!!!!!!!!!!"
1922 BEEP
1930 FOR LOOP = 1 TO NCONVERSIONS#
1932 WAIT STATUS.REGISTER, READ.WAIT
1934 ADL(LOOP) = INP(DATA.REGISTER)
1936 WAIT STATUS.REGISTER, READ.WAIT
1938 ADH(LOOP) = INP(DATA.REGISTER)
1940 '
1941 'AT THE END OF EACH 4 CHANNEL SERIES, LOOP CONVERTS HIGH AND LOW BYTES
1942 'INTO UNITS (MM AND N), THEN USES THESE TO COMPUTE AND PRINT CURRENT MOMENT
1943 '
1950 IF LOOP/4 = INT(LOOP/4) THEN 1952 ELSE 1980
1952 DELTA.H = ((((ADH(LOOP-3) * 256 + ADL(LOOP-3)) - (ADH(1) * 256 + ADL(1)))
                                        * .002441) * 2) * 3.056
1954 TENSION! = ((((ADH(LOOP-1) * 256 + ADL(LOOP-1)) * .002441) * 2 -10) -
     VOLTAGE!) *263.01
1956 HFORCE! = ((((ADH(LOOP) * 256 + ADL(LOOP)) - (ADH(4) * 256 + ADL(4))) *
     .002441) * 2) * 8.693
1958 MOMENT! = (HFORCE! * 783.18) - (TENSION! * DELTA.H)
1960 TRUEPSI! = MOMENT!/1068.77
1962 ADJPSI! = TARGET! - TRUEPSI!
```

```
1963 '
1964 '
1966 PRINT USING"############.#";ADJPSI!;MOMENT!
1980 NEXT LOOP
1990 '
1991 PRINT "!!!!!!DATA COLLECTION COMPLETE - CONVERSION IN PROGRESS !!!!!!!!"
1992 BEEP
1993 BEEP
2000 'WAIT UNTIL THE DT2801 BOARD READY FLAG IS SET, INDICATING COMMAND
2010 'COMPLETION, THEN CHECK THE STATUS REGISTER ERROR FLAG.
2020 '
2030 WAIT STATUS.REGISTER, COMMAND.WAIT
2040 STATUS = INP(STATUS.REGISTER)
2050 IF (STATUS AND &H80) THEN GOTO 3450
2060 '
2090 '
2110 FACTOR# = (10/BASE.FACTOR#) / GAIN(ADGAIN)
2140 '
2145 'CREATE AN ARRAY TO CONTAIN RAW DATA (RAW)
2147 DIM RAW!(4200)
2150 FOR LOOP = 1 TO NCONVERSIONS#
2160 '
2170 'CALCULATE THE A/D READING IN VOLTS.
2180 '
2190 DATA.VALUE# = ADH(LOOP) * 256 + ADL(LOOP)
2200 UNI.VOLTS# = DATA.VALUE# * FACTOR#
2230 BI.VOLTS#=UNI.VOLTS# * 2 - (10/GAIN(ADGAIN))
2235 RAW!(LOOP) = BI.VOLTS#
2240 NEXT LOOP
3070 NCYCLE=NCONVERSIONS#/NCHAN
3080 OPEN "B:DATA"+NRUN$ FOR OUTPUT AS #1
3081 '
3082 '
3090 PRINT USING "TARGET PRESSURE IS ##.# PSI";TARGET!
3091 PRINT
3092 PRINT "      LVDT(H)      LVDT(V)    T LOAD       HOR. LOAD        TIME"
3093 PRINT "        mm           mm          N             N             secs"
3094 PRINT
3095 PRINT #1, USING "TARGET PRESSURE IS ##.# PSI";TARGET!
3096 PRINT #1,
3097 PRINT #1,"      LVDT(H)      LVDT(V)    T LOAD       HOR. LOAD        TIME"
3098 PRINT #1,"        mm           mm          N             N             secs
3099 PRINT #1,
3110 'START LOOP TO CONSIDER DATA for each cycle
3120 FOR CYCLEN = 1 TO NCYCLE
3130 'CALCULATE PREVAILING ELAPSED TIME
3140 TIME!=CYCLEN *.15 * NCHAN
3150 SEN1! = 3.056                'LVDT 464, HORIZONTAL DISPL. (mm/V)
3155 SEN2! = .472                 'LVDT 1406, VERTICAL DISPL. (mm/V)
3160 SEN3! = 263.01               'LOAD CELL, TENSION (N)
3165 SEN4! = 8.6926               'PRESSURE TRANSDUCER, HOR. FORCE (N)
3170 FOR CHANN = 1 TO NCHAN
3175 VN! = RAW!(((CYCLEN-1)*NCHAN)+CHANN)
3180 IF (CHANN=1)THEN SEN!=SEN1!:ZERO!=RAW!(1)
```

```
3185 IF (CHANN=2)THEN SEN!=SEN2!:ZERO!=RAW!(2)
3190 IF (CHANN=3)THEN SEN!=SEN3!:ZERO!=VOLTAGE!
3195 IF (CHANN=4)THEN SEN!=SEN4!:ZERO!=RAW!(4)
3200 RES!=(VN!-ZERO!)*SEN!
3205 PRINT #1, USING "#######.####,";RES!,
3206 PRINT USING "#######.####";RES!,
3210 NEXT CHANN
3212 PRINT #1, USING "#########.##,";TIME!,
3214 PRINT USING "#########.##";TIME!,
3215 PRINT #1,
3216 PRINT
3220 NEXT CYCLEN
3417 PRINT "S E Q U E N C E   C O M P L E T E  ! ! !"
3440 GOTO 3480
3450 PRINT
3460 PRINT "error IN PROGRAM"
3461 OUT COMMAND.REGISTER,CSTOP
3462 DMY=INP(DATA.REGISTER)
3463 WAIT STATUS.REGISTER,COMMAND.WAIT
3464 OUT COMMAND.REGISTER,&H2
3466 WAIT STATUS.REGISTER,READ.WAIT
3467 PRINT "lowbyte error = " INP(DATA.REGISTER)
3468 WAIT STATUS.REGISTER,READ.WAIT
3469 PRINT "highbyte error = " INP(DATA.REGISTER)
3470 PRINT "DO YOU WANT TO CONTINUE (Y OR N)?";
3471 INPUT ANSWER$
3472 IF (ANSWER$ = "Y") GOTO 2110
3480 END
```

APPENDIX B

Analysis of variance for the data from the wafer technique is presented below.

Tensile Load to Failure Data
(Newtons)

	Bending Moment Level				
	0	3	4	5	Average
Wafer Config.	927.0	597.6	560.0	0	
	934.1	451.8	437.6	0	
L-R	901.2	964.7	451.8	0	542.6
	983.5	818.8	487.1	167.1	
AVG.	936.5	708.2	484.1	41.8	
	948.4	899.1	784.1	345.1	
V-R	1000.0	870.9	864.5	387.3	783.3
	964.8	943.7	889.7	504.7	
AVG.	971.1	904.3	845.1	412.4	
	731.9	527.3	407.4	0	
L-T	737.2	502.6	236.3	0	392.8
AVG.	734.6	515.0	321.9	0	
Average	903.1	730.7	568.4	156.0	

ANOVA - Tensile Load to Failure

Source	D.F.	Sequential Sum of Squares	Mean Square	Sequential F-ratio	Tail Prob
A	2	795111.4	397555.7	41.82	0.00
B	2	2759818	919939.3	96.77	0.00
AB	6	143511	23918.5	2.52	0.05
Model	11	3698441	336221.9	35.37	0.00
Error	24	228163	9506.8		
Adj Total	35	3926604	112188.7		

Slope of the Load-Slip Curves
(Newtons/mm)

	Bending Moment Level				
	0	3	4	5*	Average
Wafer Config.	1184.35	874.0	904.21		
	1215.11	959.47	1030.48		
L-R	804.37	1333.59	910.73		1050.97
	1238.55	1107.89	1048.85		
AVG.	1110.60	1068.74	937.57		
	963.06	870.4	911.98	569.59	
V-R	973.93	903.64	935.93	734.42	943.46
	985.88	894.86	1051.48	916.30	
AVG.	974.29	889.63	966.46		
	617.33	531.16	630.17		
L-T	530.11	574.29	614.67		582.96
AVG.	537.72	552.73	622.42		
Average	945.85	894.37	893.17		

* Data from this moment level was not used in calculations

ANOVA - Tensile Load to Failure

Source	D.F.	Sequential Sum of Squares	Mean Square	Sequential F-ratio	Tail Prob
A	2	890252.9	445126.4	28.36	0.00
B	2	16285.3	8142.65	0.52	0.53
AB	4	41406.69	23918.5	2.52	0.05
Model	8	997944.9	118493.1	7.55	0.00
Error	18	282553.2	15697.4		
Adj Total	26	1230498	47326.85		